The Plant Cell, Vol. 19: 3170–3193, October 2007, www.plantcell.org

Proteome Analysis of *Arabidopsis* Leaf Peroxisomes Reveals Novel Targeting Peptides, Metabolic Pathways, and Defense Mechanisms [W]

Sigrun Reumann,[a,1,2] Lavanya Babujee,[a,3] Changle Ma,[a,4] Stephanie Wienkoop,[b] Tanja Siemsen,[a] Gerardo E. Antonicelli,[a,5] Nicolas Rasche,[a] Franziska Lüder,[a,6] Wolfram Weckwerth,[b,c] and Olaf Jahn[d,e]

[a] Department of Plant Biochemistry, Georg-August-University of Goettingen, Albrecht-von-Haller-Institute for Plant Sciences, D-37077 Goettingen, Germany

[b] Max-Planck-Institute of Molecular Plant Physiology, Metabolic Networks, D-14424 Potsdam, Germany

[c] University of Potsdam, Institute of Biochemistry and Biology, 14469 Potsdam, Germany

[d] Max-Planck-Institute of Experimental Medicine, Proteomics Group, D-37075 Goettingen, Germany

[e] Deutsche Forschungsgemeinschaft Research Center for Molecular Physiology of the Brain, D-37073 Goettingen, Germany

We have established a protocol for the isolation of highly purified peroxisomes from mature *Arabidopsis thaliana* leaves and analyzed the proteome by complementary gel-based and gel-free approaches. Seventy-eight nonredundant proteins were identified, of which 42 novel proteins had previously not been associated with plant peroxisomes. Seventeen novel proteins carried predicted peroxisomal targeting signals (PTS) type 1 or type 2; 11 proteins contained PTS-related peptides. Peroxisome targeting was supported for many novel proteins by in silico analyses and confirmed for 11 representative full-length fusion proteins by fluorescence microscopy. The targeting function of predicted and unpredicted signals was investigated and SSL>, SSI>, and ASL> were established as novel functional PTS1 peptides. In contrast with the generally accepted confinement of PTS2 peptides to the N-terminal domain, the bifunctional transthyretin-like protein was demonstrated to carry internally a functional PTS2. The novel enzymes include numerous enoyl-CoA hydratases, short-chain dehydrogenases, and several enzymes involved in NADP and glutathione metabolism. Seven proteins, including β-glucosidases and myrosinases, support the currently emerging evidence for an important role of leaf peroxisomes in defense against pathogens and herbivores. The data provide new insights into the biology of plant peroxisomes and improve the prediction accuracy of peroxisome-targeted proteins from genome sequences.

INTRODUCTION

Peroxisomes are ubiquitous cell organelles that compartmentalize primarily oxidative metabolic reactions. A characteristic of peroxisomes is their metabolic flexibility because their enzymatic constituents vary depending on the organism, the type of tissue, and the environmental conditions (for review, see Beevers, 1979; Hayashi and Nishimura, 2006). Plant peroxisomes differentiate into tissue- and developmental-specific variants, such as leaf peroxisomes in mature leaves and glyoxysomes in germinating seeds, and typically participate in metabolic pathways and networks that are spread over multiple subcellular compartments. For instance, the recycling of 2-phosphoglycolate during photorespiration requires orchestration of 15 chloroplastic, peroxisomal, and mitochondrial enzymes and numerous transport proteins to transfer the intermediates between cell compartments (for review, see Reumann, 2002; Reumann and Weber, 2006). Similarly, fatty acids are released from lipid bodies during seed germination and transferred to glyoxysomes, where the carbon chain is transformed into sucrose in coordination with mitochondrial and cytosolic enzymes. Compartmentalization of hydrogen peroxide–producing oxidases in peroxisomes offers the advantage that H_2O_2 and other reactive oxygen species (ROS) can immediately be detoxified at the site of production by catalase (CAT) and auxiliary antioxidative enzymes (for review, see del Rio et al., 2006). In addition to these basic metabolic functions, a role for peroxisomes in the biosynthesis of the plant hormone auxin and the signaling molecule jasmonic acid (JA) and in sulfur and nitrogen metabolism has been established

[1] Current address: Department of Molecular, Cellular, and Developmental Biology, University of Michigan, 830 North University Avenue, Ann Arbor, MI 48109 and Michigan State University–Department of Energy Plant Research Laboratory, East Lansing, MI 48824-1312.

[2] Address correspondence to sreuman@gwdg.de.

[3] Current address: Department of Plant Pathology, Faculty of Agriculture, Shizuoka University, Shizuoka 422-8529, Japan.

[4] Current address: Section of Molecular Biology, Division of Biological Sciences, University of California, San Diego, La Jolla, CA 92093.

[5] Current address: Biochemistry Department, Clemens Schöpf Institute, Technical University of Darmstadt, Petersenstraβe 22, D-64287, Darmstadt, Germany.

[6] Current address: Department of Biochemistry and Molecular Biology, Bio21 Molecular Science and Biotechnology Institute, University of Melbourne, 30 Flemington Road, Parkville, Victoria 3010, Australia.

The author responsible for the distribution of materials integral to the findings presented in this article in accordance with the policy described in the Instructions for Authors (www.plantcell.org) is: Sigrun Reumann (sreuman@gwdg.de).

[W] Online version contains Web-only data.

www.plantcell.org/cgi/doi/10.1105/tpc.107.050989

(Zolman et al., 2001; Strassner et al., 2002; Nowak et al., 2004; Koo et al., 2006). Moreover, evidence is emerging from recent studies that peroxisomes not only have important functions in metabolism but also play an essential role in specific defense mechanisms conferring resistance against pathogen attack (Taler et al., 2004; Koh et al., 2005; Lipka et al., 2005).

Thanks to rapid advances in genome sequencing, the potential of computational approaches is increasingly being realized to predict peroxisomal proteins and explore the biology of plant peroxisomes. In silico analyses take advantage of conserved targeting sequences in peroxisomal proteins (i.e., the C- terminal tripeptide constituting the peroxisomal targeting signal type 1 [PTS1] of the prototype SKL> [> designates the extreme C terminus] or the cleavable PTS2 nonapeptide located in the N-terminal domain [prototype RLx_5HL]) to predict targeting of unknown proteins to peroxisomes (Emanuelsson et al., 2003; Kamada et al., 2003; Neuberger et al., 2003a, 2003b; Reumann, 2004; Hawkins and Boden, 2006). Except for few proteins (e.g., plant CAT and *Arabidopsis thaliana* sarcosine oxidase; Kamigaki et al., 2003; Goyer et al., 2004), all known matrix proteins from plant peroxisomes carry either a C-terminal PTS1 or an N-terminal PTS2 (Reumann, 2004). Plant PTS motifs have been defined by experimental and bioinformatics approaches and yielded partially overlapping results but differed in specificity and peptide identity. A relatively large number (24 to 120) of PTS1 peptides have been suggested to target proteins to peroxisomes in higher plants (Hayashi et al., 1997; Mullen et al., 1997; Kragler et al., 1998), but experimental limitations required data extrapolation from amino acid substitutions to all possible residue combinations within the three-residue motif and thereby reduced motif specificity. By in silico analysis of plant EST databases (Reumann, 2004), nine major and 11 minor PTS1 peptides were defined according to stringent criteria and thus considered as rather specific, though certainly yet incomplete. A search of the *Arabidopsis* genome for proteins carrying these peptides revealed 280 putative PTS1/2 proteins listed in the database AraPerox (Reumann et al., 2004; www.araperox.uni-goettingen.de). Despite considerable progress, prediction by PTSs is still limited by the low number of PTS-containing proteins that have been characterized at the molecular level, at least in one plant species (18 PTS1 and 14 PTS2 proteins; Reumann, 2004). However, the predictive algorithms for PTS1 proteins in particular can steadily be improved, as 12 additional proteins with putative PTS1s have been shown to be targeted to peroxisomes in the past 3 years and, at least in some cases, have been demonstrated to follow the PTS1 targeting pathway. The recently cloned cDNAs encode, for instance, auxiliary enzymes of fatty acid β-oxidation, ROS metabolism, and JA activation, and one of two small heat shock proteins (sHsps); the second sHsp is the only additional PTS2 protein (Edqvist et al., 2004; Tilton et al., 2004; Goepfert et al., 2005, 2006; Leterrier et al., 2005; Lisenbee et al., 2005; Schneider et al., 2005; Turner et al., 2005; Koo et al., 2006; Ma et al., 2006; Helm et al., 2007; Zolman et al., 2007).

Taken together, the low number of well-characterized plant peroxisomal matrix proteins leads to four principal constraints limiting in silico predictions of peroxisomal PTS1/2 proteins: (1) insufficient coverage of functional targeting peptides, (2) limited knowledge of the identity and function of auxiliary targeting elements surrounding the short PTS peptides, (3) possible dominance of N-terminal nonperoxisomal targeting signals over C-terminal PTS1s, and (4) unpredictable masking of PTS surface exposure by polypeptide conformation, homo- and hetero-oligomerization, or posttranslational regulatory mechanisms. Thus, the currently available prediction tools suffer from both insufficient sensitivity (i.e., an incomplete detection of true PTS1/2 proteins) and insufficient specificity (i.e., the identification of a significant number of false positives). Notably, many proteins of peroxisomes cannot currently be predicted from genome sequences at all, including peripheral and integral membrane proteins, subunits that are imported into the matrix in a piggy-backed fashion, and matrix proteins with internal PTS1-like peptides (e.g., yeast acyl-CoA oxidase and plant CAT; Klein et al., 2002; Kamigaki et al., 2003).

In the postgenomic era of plant peroxisomal research, a major challenge is the identification and functional characterization of plant-specific proteins. Many of the recently cloned cDNAs of plant peroxisomal proteins have been identified by computational homology analysis using the protein sequence of peroxisomal enzymes from mammals or fungi as query (Edqvist et al., 2004; Tilton et al., 2004; Goyer et al., 2004; Goepfert et al., 2005, 2006). Even though proven to be successful, this approach fails by definition to unravel plant-specific proteins. Instead, systematic large-scale experimental studies of plant peroxisomes are required. Technical advances in two-dimensional gel electrophoresis (2-DE), liquid chromatography (LC), and mass spectrometry (MS) laid the foundation for the progress in organellar proteome studies (for review, see Taylor et al., 2003; Peck, 2005; Glinski and Weckwerth, 2006) and for cell-specific profiling (Wienkoop et al., 2004). The major bottleneck of organellar proteomics is the purity of the cell compartment of interest. With respect to their fragile nature, the isolation of intact peroxisomes in high purity is difficult irrespective of the source organism but is even more challenging in plants, mainly due to the predominance of plastids as another contaminating cell compartment and a myriad of secondary metabolites with organelle-destabilizing effects in vitro. For these reasons, the first proteome studies of peroxisomes have only recently been reported (for review, see Saleem et al., 2006). As the availability of complete genome information or large EST collections is a prerequisite for straightforward protein identification and because peroxisome isolation protocols are hardly interchangeable between plant species, such proteome studies were hampered by the fact that the isolation of plant peroxisomes in high purity was restricted to few plant species (e.g., *Pisum sativum* and *Spinacia oleracea*), which lacked genome or EST sequence information. Complete genome analysis of *Arabidopsis* (Arabidopsis Genome Initiative, 2000) rendered this tiny weed the species of choice for proteome studies of plant peroxisomes, provided that the organelles could be isolated in sufficient purity and quantity. Initial proteome analyses of leaf peroxisomes and glyoxysomes from greening and etiolated *Arabidopsis* cotyledons have been reported, but probably due to insufficient organelle purity and/or technical limitations in protein identification, only few known and novel PTS-containing proteins have been identified (Fukao et al., 2002, 2003). Leaf peroxisomes are considered the variant of choice for a comprehensive long-term

project aimed at the identification and functional analysis of all plant-specific proteins from peroxisomes because mature leaves are (1) physiologically the most significant plant tissue (site of photosynthesis, photorespiration, numerous biosynthetic pathways, and nitrogen and sulfur assimilation); (2) the most distinctive tissue of plants compared with yeast and mammals; and (3) second only to roots, the major plant organ that interacts with the environment (i.e., that perceives and immediately reacts to stress, both abiotic [high light, extreme temperature, drought, and hail] and biotic [pathogen and herbivore attack]).

With the objective to verify and ultimately improve the prediction accuracy of plant peroxisomal proteins from genome sequences, we applied the unbiased large-scale approach of organellar proteomics to leaf peroxisomes. A purification method was developed for leaf peroxisomes from mature *Arabidopsis* leaves in high purity by Percoll and sucrose density gradient centrifugation. Protein separation by 2-DE in combination with peptide mass fingerprinting (PMF) and peptide fragment fingerprinting supplemented by a gel-free shotgun approach led to the identification of 36 known and 42 novel peroxisomal proteins. Peroxisome targeting of the novel PTS-containing proteins was corroborated by the conservation of PTSs in orthologs of higher plants as revealed by analysis of protein and EST databases. By fluorescence microscopy, peroxisome targeting of 11 representative proteins carrying predicted PTS or PTS-related peptides was verified for fusion proteins with enhanced yellow fluorescent protein (EYFP) in onion epidermal cells. Thereby, three novel PTS1 tripeptides (SSL>, SSI>, and ASL>) and an internal PTS2 were established, providing valuable input for further development of prediction tools. The novel plant peroxisomal proteins indicate that leaf peroxisomes play an important role in catabolism of complex metabolites, in biosynthetic pathways, and in defense mechanisms against pathogens and herbivores.

RESULTS

Isolation of Peroxisomes from Mature *Arabidopsis* Leaves in High Purity

To identify plant-specific peroxisomal proteins by a large-scale proteomics approach, a new isolation method for leaf peroxisomes from *Arabidopsis* was established with the objectives of (1) increasing the stability of peroxisomes in aqueous solution, (2) reducing the physical interaction of peroxisomes with mitochondria and chloroplasts, a pronounced phenomenon in *Brassicaceae*, and (3) increasing the specificity of peroxisome enrichment by a combination of Percoll and sucrose density gradient centrifugation. To this end, 3- to 4-week-old plants were harvested at the end of the dark period and gently ground in a buffer of high osmolarity. After separation of intact chloroplasts, but notably without peroxisome sedimentation by differential centrifugation, the supernatant was laid directly on top of a discontinuous Percoll density gradient (Figure 1A). Cosedimentation of peroxisomes along with mitochondria and thylakoid membranes by differential centrifugation prior to isopycnic organelle separation increased irreversibly interorganellar adhesion and peroxisome contamination. Whereas chloroplasts, thylakoid membranes, and mitochondria were largely retained in the 15 and 38% (v/v) Percoll fraction near the top of the gradient, intact leaf peroxisomes passed the Percoll layer and were recovered at the bottom, visible as a whitish diffuse organelle sediment (Figures 1B and 1C; see Supplemental Figure 1 online). Peroxisome fractions of several Percoll gradients were combined and washed in Tricine/EDTA buffer containing 36% (w/w) sucrose. Approximately 7% of total activity of the leaf peroxisomal marker enzyme hydroxypyruvate reductase (HPR) of the crude extract was recovered in the first fraction of leaf peroxisomes (LP-P1) with a yield of ~90 nkat HPR per 60 g fresh weight (Table 1). The peroxisome fraction was carefully homogenized and laid on top of a discontinuous sucrose density gradient (Figure 1D; see Supplemental Figure 1 online). After ultracentrifugation, intact leaf peroxisomes were enriched close to the bottom of the gradient, visible as a sharp white band, at the typical density of plant peroxisomes of ~50 to 53% (w/w) sucrose (Figures 1E and 1F; see Supplemental Figure 1 online). Even though only half of the peroxisomes could be recovered, the contamination by chloroplasts and mitochondria was further reduced by a factor of three (Table 1). On average, 115 ± 29 μg protein were obtained with a specific HPR activity of 293 ± 76 nkat/mg protein (Table 1). The purity of leaf peroxisomes was high, as determined by the activities of marker enzymes for leaf peroxisomes (HPR), mitochondria (fumarase), and chloroplasts (NADP-dependent glyceraldehyde-3-phosphate dehydrogenase [GAPDH]) and the content of chlorophyll (thylakoids); contaminating chloroplasts and mitochondria were estimated to comprise only 0.1 and 1.7% of the total, respectively (Table 1).

Identification of Proteins from Mature Leaf Peroxisomes

Peroxisome fractions of highest purity (~400 nkat HPR/mg protein) were analyzed by 2-DE to display the proteinaceous constituents of *Arabidopsis* leaf peroxisomes as maps of intact proteins (Figure 2). Upon gel staining with colloidal Coomassie blue, ~180 separated protein spots were visualized, out of which 135 were identified with high confidence by peptide mass and fragment fingerprinting, using an automated platform based on matrix-assisted laser desorption/ionization time-of-flight mass spectrometry (MALDI-TOF-MS) (Jahn et al., 2006). Summarized over several two-dimensional gels, in addition to 28 known plant peroxisomal proteins, 36 proteins were identified that had previously not been associated experimentally with plant peroxisomes and are referred to as novel proteins throughout this study.

With respect to peroxisome purity, few minor spots derived from dominant proteins of chloroplasts and mitochondria. For instance, the presence of the large and small subunits of ribulose-1,5-bisphosphate carboxylase/oxygenase, the most abundant plant protein, and small subunits of the photosystems (e.g., PSBP; Figure 2) indicated a low contamination with chloroplasts. Similarly, a few tiny protein spots represented mitochondrial proteins, including the P and H subunits of Gly decarboxylase (GDC-P and GDC-H), which is the most prominent mitochondrial protein; subunit β of the ATP synthase complex (ATPase β); and Ser-hydroxymethyltransferase (Figure 2). By contrast, no dominant proteins were detected of the endoplasmic reticulum (ER) (e.g., BiP), the nucleus (e.g., histones and

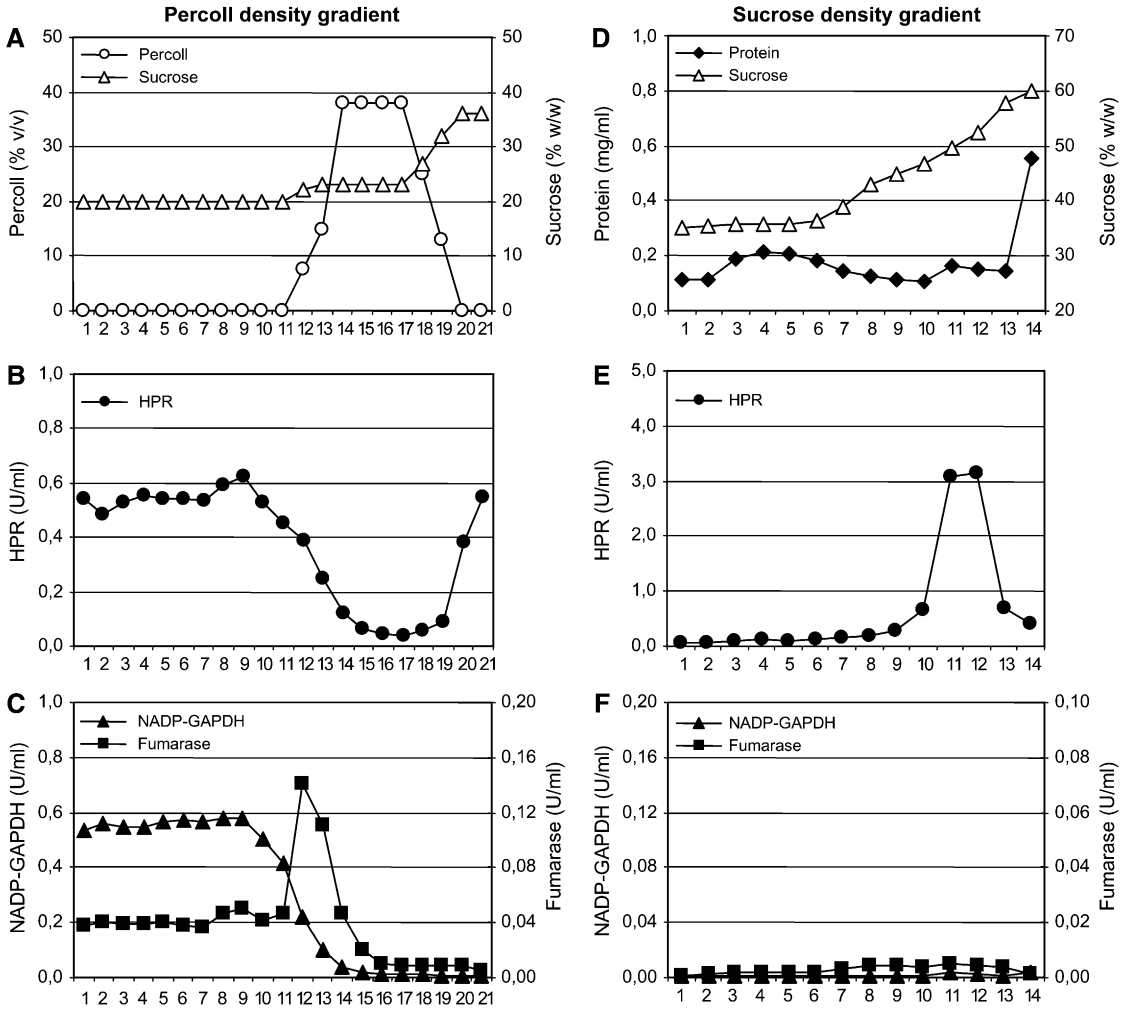

Figure 1. Isolation of Peroxisomes from Mature *Arabidopsis* Leaves.

The supernatant of the chloroplast sedimentation was loaded on top of a discontinuous Percoll gradient underlaid with fractions of increasing sucrose concentration **(A)**. The Percoll concentrations refer to the concentrations prior to gradient centrifugation. After centrifugation, the Percoll gradient was fractionated from the top to the bottom into 21 2-mL fractions and analyzed for organellar marker enzyme activities, namely HPR (leaf peroxisomes) **(B)**, fumarase (mitochondria), and NADP-dependent GAPDH (chloroplasts) **(C)**. After washing, the peroxisome fractions of eight Percoll gradients were combined and homogenized, and the resuspension was laid on top of a discontinuous sucrose density gradient followed by ultracentrifugation. After fractionation from the top to the bottom into 14 1-mL fractions, the concentrations of protein and sucrose were determined **(D)**. Marker enzyme activities were analyzed as before (**[E]** and **[F]**). Note that the scale between the first and second density gradients is increased by a factor of 5 for HPR and decreased for NADP-GAPDH (factor 5) and fumarase (factor 2).

DNA polymerase subunits), the plasma or tonoplast membranes, or the Golgi. Likewise, major cytosolic proteins were not found except for two spots identified as cytosolic glyceraldehyde phosphate dehydrogenase subunit C and aconitase. Based on the staining intensity of leaf peroxisomal versus nonperoxisomal protein spots (Figure 2), we concluded that leaf peroxisomes were isolated at ~95% purity, with a minor contamination by dominant proteins from mitochondria and chloroplasts but not by other subcellular compartments.

Although two-dimensional gel-based proteomics approaches offer the advantage that protein integrity and information on protein abundance, isoform identity, and posttranslational modifications are retained, limitations with respect to the identification of small, basic, and hydrophobic proteins are reported. To complement the gel-based approach and improve coverage of the peroxisomal proteome, a gel-free technique was added that employs one-dimensional LC separation at the level of proteolytic peptides, commonly referred to as the shotgun approach (Link et al., 1999). This technique is very sensitive and requires only small amounts of total protein, as demonstrated recently by cell-specific protein profiling in pooled trichome and epidermis cells from *Arabidopsis* (Wienkoop et al., 2004). The proteins identified by this method largely overlapped with those of the gel-based approach; however, additionally, eight known and

Table 1. Biochemical Analysis of Peroxisome Purity

	HPR		NADP-Dependent GAPDH			Fumarase		
	Activity (nkat)	Percentage of CE	Activity (nkat)	Percentage of CE	Contamination (%)	Activity (nkat)	Percentage of CE	Contamination (%)
Crude extract	1240 ± 70	100	1500 ± 500	100		167 ± 35	100	
Leaf peroxisome fraction LP-P1	89.5 ± 27.5	7.2	0.39 ± 0.14	0.026	0.36	0.56 ± 0.32	0.33	4.6
Leaf peroxisome fraction LP-P2	45.8 ± 17.5	3.7	0.065 ± 0.029	0.0043	0.12	0.10 ± 0.04	0.062	1.7

Peroxisome purity was determined on the basis of marker enzyme activities specific for leaf peroxisomes (HPR), chloroplasts (NADP-dependent GAPDH), and mitochondria (fumarase). The protein content of the leaf peroxisomal fraction LP-P2 was 115 ± 29 μg, resulting in a specific HPR activity of 293 ± 76 nkat/mg protein and a yield of 1.9 ± 0.5 μg protein/g fresh weight. The content of chlorophyll (thylakoids) was below the limits of detection in both leaf peroxisomal fractions LP-P1 and P2 (data not shown) ($n = 5$). CE, crude extract.

six novel proteins were detected only by the shotgun strategy. These proteins generally had either a basic isoelectric point (pI > 8.4) and/or were small proteins (<150 residues), underscoring the complementary nature of the two approaches applied. In total, we identified 78 nonredundant proteins, comprising 36 known and 42 novel proteins (Table 2; see Supplemental Table 1 online). Filtered mass spectra for protein identifications are stored in ProMEX, a mass spectral reference library for plant proteomics, that can be searched with peptide product ion spectra of unknown samples (Hummel et al., 2007).

Known Plant Peroxisomal Proteins

Identified proteins already known as constituents of leaf peroxisomes or glyoxysomes in any plant species are listed in Supplemental Table 1 online. As valuable information on protein

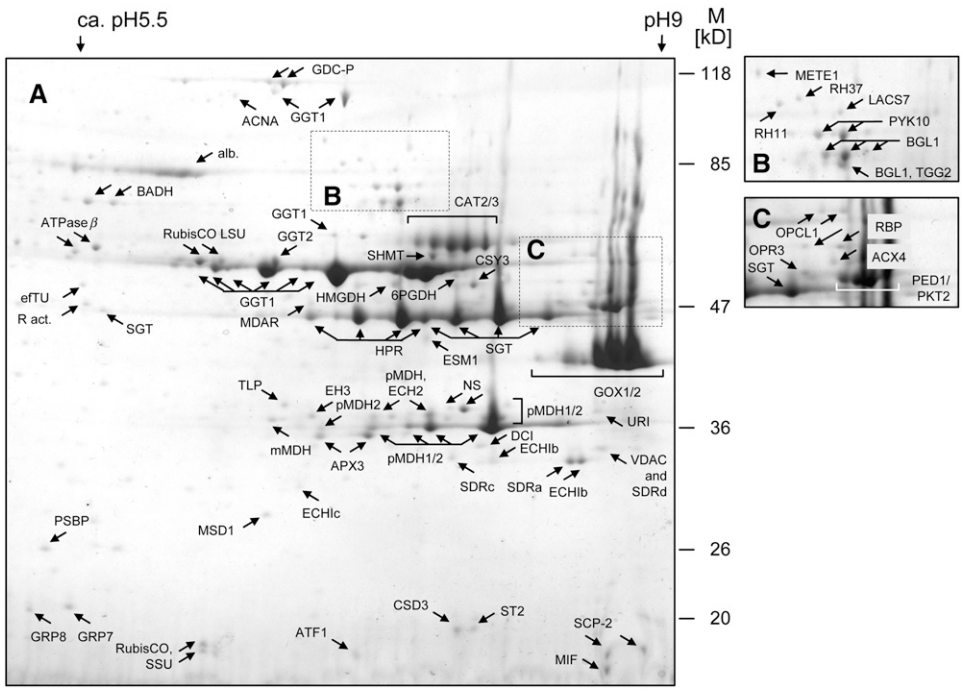

Figure 2. Two-Dimensional Protein Map of Isolated Leaf Peroxisomes from *Arabidopsis*.

Leaf peroxisomal proteins (200 μg) of a specific HPR activity of 400 nkat HPR/mg protein were first separated according to pI by isoelectric focusing on commercial IPG strips (18 cm, nonlinear, pH 3.0 to 10) followed by SDS-PAGE on 10 to 15% (w/v) acrylamide gradient gels **(A)**. For the sake of clarity, the annotations of the protein spots within the dashed frames are shown magnified in **(B)** and **(C)**. Proteins were visualized by colloidal Coomassie blue staining. Stained proteins were excised manually and subjected to an automated platform for protein identification (Jahn et al., 2006). Two artificial Coomassie spots caused by dye crystals were eliminated from the figure. Abbreviations not listed in Supplemental Table 1 online or Table 2 are as follows: ACNA, (cytosolic) aconitase; alb., BSA; ATPase β, ATP synthase subunit β; efTU, elongation factor TU; GDC-P, Gly decarboxylase P protein; PSBP, oxygen-evolving enhancer protein 2; RubisCO LSU and SSU, ribulose-1,5-bis-phosphate carboxylase/oxygenase large and small subunits; SHMT, Ser-hydroxymethyltransferase; VDAC, voltage-dependent anion-selective channel.

Table 2. Novel Proteins Identified in *Arabidopsis* Leaf Peroxisomes

Abbreviation	Protein	Gene Locus	Predicted Targeting Signals	Approach of Protein Identification		PTS1/2	PTS Conservation	Peroxisomal EYFP Fusion Protein Targeting
				Gel-Based	Shotgun			
β-Oxidation–related annotation								
AAE5	Acyl-activating enzyme 5	At5g16370		Yes	ND	SRM>	ND[4]	Not det.
ECHIa	Monofunctional enoyl-CoA hydratase/ isomerase isoform a	At4g16210		ND	Yes	SKL>[6]	Yes[4]	Yes[6]
ECHIb	Monofunctional enoyl-CoA hydratase/ isomerase isoform b/carnitine racemase	At4g14430		Yes	Yes	PKL>[4]	Yes[4]	Yes[4]
ECHIc	Monofunctional enoyl-CoA hydratase/ isomerase isoform c/carnitine racemase	At1g65520		Yes	ND	SKL>	Yes[4]	Not det.
NS/ECHId	Naphthoate synthase	At1g60550		Yes	Yes	RLx$_5$HL[6]	Yes[4]	Yes[6]
HBCDH	Hydroxybutyryl-CoA dehydrogenase	At3g15290		Yes	ND	PRL>[4]	Yes[5]	Yes[4]
ST2	Small thioesterase isoform 2	At1g04290		Yes	ND	SNL>	Yes[4]	Not det.
SDRa	Short-chain dehydrogenase/ reductase isoform a	At4g05530		Yes	Yes	SRL>[6]	Yes[4]	Yes[6]
SDRb/ DECR	Short-chain dehydrogenase/ reductase isoform b	At3g12800		Yes	NS[2]	SKL>[4]	Yes[5]	Yes[4]
SDRc	Short-chain dehydrogenase/ reductase isoform c	At3g01980		Yes	NS[2]	(SYM>)	ND	Not det.
SDRd	Short-chain dehydrogenase/ reductase isoform d	At3g55290		Yes	ND	SSL>[3]	ND[4]	Not det.
BSMDR/ARP	Bifunctional short- and medium-chain dehydrogenase/reductase (Arg-rich protein)	At1g49670		ND	Yes[1]	SRL>	Yes[4]	Not det.
EH3	Epoxide hydrolase isoform 3	At4g02340		Yes	ND	ASL>[3, 4]	ND [4]	Yes[4]
ACAT2	Acetoacetyl-CoA thiolase 2	At5g48230		Yes	ND	ND	Yes[4]	Not det.
GOX3	Glycolate oxidase isoform 3	At4g18360		ND	Yes[1]	AKL>	ND [4]	Not det.
IDH	NADP-dependent isocitrate dehydrogenase	At1g54340		Yes	ND	SRL>[4]	Yes[5]	Yes[4]
6PGDH	Phosphogluconate dehydrogenase	At3g02360		Yes	ND	SKI>[4]	Yes[5]	No[4*]
6PGL	6-Phosphogluconolactonase	At5g24400	TP	ND	ND	SKL>[4]	Yes[5]	Yes[4]
Detoxification								
GR	Glutathione reductase	At3g24170		Yes	ND	(TNL>)	ND[4]	Not det.
GSTT1	Glutathione *S*-transferase, isoform θ 1	At5g41210		ND	Yes	SKI>[4]	Yes[4]	Yes[4]
HMGDH	*S*-(Hydroxymethyl)glutathione dehydrogenase (GSH-FDH)	At5g43940		Yes	ND	ND	NA	Not det.
Pathogen and herbivore defense								
BGL1	β-Glucosidase 1	At1g52400	SP, RS	Yes	Yes	ND	NA	Not det.
PYK10	β-Glucosidase PYK10	At3g09260	SP, RS	Yes	Yes[1]	ND	NA	Not det.
TGG1	Myrosinase, thioglucosidase 1	At5g26000	SP	Yes	ND	ND	NA	Not det.
TGG2	Myrosinase, thioglucosidase 2	At5g25980	SP	Yes	ND	ND	NA	Not det.
ESM1	Epithiospecifier modifier 1 (myrosinase-associated protein)	At3g14210	SP	Yes	ND	ND	NA	Not det.
MIF	Macrophage migration inhibitory factor	At3g51660		Yes	ND	SKL>	Yes[4]	Not det.
OZI1	Ozone-induced protein 1	At4g00860	(SP)	ND	Yes	ND	NA	Not det.
Nucleic acid metabolism								
GRP7	Gly-rich protein isoform 7	At2g21660		Yes	Yes	ND	NA	Not det.
GRP8	Gly-rich protein isoform 8	At4g39260		Yes	Yes	ND	NA	Not det.
RH11	DEAD-box RNA helicase 11	At3g58510	(TP)	Yes	ND	ND	NA	Not det.
RH37	DEAD-box RNA helicase 37	At2g42520	TP	Yes	ND	ND	NA	Not det.
RBP	RNA binding protein	At4g17520		Yes	ND	ND	NA	Not det.
NBP	Nucleotide binding protein	At4g16566		ND	Yes	(SKV>)	ND[4]	Not det.

(Continued)

Table 2. (continued).

Abbreviation	Protein	Gene Locus	Predicted Targeting Signals	Approach of Protein Identification		PTS1/2	PTS Conservation	Peroxisomal EYFP Fusion Protein Targeting
				Gel-Based	Shotgun			
Other annotated functions								
OASS A1	*O*-Acetylserine sulfhydrylase isoform A1	At4g14880		Yes	ND	ND	NA	Not det.
METE1	Cobalamin-independent Met synthase	At5g17920		Yes	ND	(SAK>)	ND[4]	Not det.
BADH	Betaine aldehyde dehydrogenase	At3g48170	(MP)	Yes	NS[2]	SKL>	ND[4]	Not det.
ATF1	Acetyl transferase isoform 1	At1g21770		Yes	ND	SSI>[3,4]	Yes[4]	Yes[4]
TLP	Transthyretin-like protein	At5g58220		Yes	ND	RLx_5HL (int.)[3,4]	Yes[4]	Yes[4]
Unknown proteins without annotation								
UP1	Unknown protein 1	At1g52410	SP	Yes	ND	SSL>[3]	ND[4]	Not det.
UP2	Unknown protein 2	At3g15950	SP	Yes	ND	(SLN>)	ND[4]	Not det.
UP3	Unknown protein 3	At2g31670	MP	Yes	ND	SSL>[3]	ND[4]	Not det.
UP4	Unknown protein 4	At1g09340		Yes	ND	ND	NA	Not det.

For 43 novel plant peroxisome proteins identified in this study (42 proteins detected in isolated leaf peroxisomes and 6PGL), abbreviation, gene locus, predicted targeting signals, the method used for protein identification (two-dimensional gel-based or shotgun approach), predicted PTS1/2 peptides, PTS conservation in homologous ESTs, and experimental data on peroxisome targeting for full-length EYFP fusion proteins are provided. The values for molecular weight and pI were calculated for the full-length polypeptides by EXPASY (www.expasy.ch/). Proteins represented by only a single peptide in the shotgun approach are indicated as significant (yes[1]) or not significant (NS[2]) for protein identification. Predicted PTS1/2s refer to a previous definition (Reumann, 2004) or to novel PTS peptides identified in this study ([3]). Novel proteins whose predicted PTS1 peptides are conserved as PTS1 peptides in homologous plant ESTs, as shown in this ([4]; see Supplemental Figure 3 online) or an earlier study ([5]; Reumann et al., 2004), are indicated. For some proteins, PTS conservation could not be analyzed owing to a lack of ESTs of high sequence similarity in plant species other than *Brassicaceae* (e.g., EH3 and UP1 to 3) or due to the presence of *Arabidopsis* paralogs of high sequence similarity lacking a PTS (e.g., AAE5, SDRd, BADH, GOX3, and METE1). PTS1-like peptides are given in parentheses. Predicted PTS peptides characterized experimentally as the targeting signals of the corresponding proteins and peroxisome targeting of full-length EYFP fusion proteins are indicated ([4], Figures 4 and 5; [6], L. Babujee, V. Wurtz, C. Ma, A. van Dorselaer, and S. Reumann, unpublished data). Even though EYFP-6PGDH (At3g02360) remained cytosolic, the enzyme is considered a true peroxisomal matrix protein (*; see Discussion). 6PGL (At5g24400) was not yet identified in isolated leaf peroxisomes but was shown to be targeted as EYFP fusion protein to peroxisomes by SKL> (Figures 4G and 4H). MP, mitochondrial presequence; RS, (ER) retention signal; SP, signal peptide; TP, transit peptide; ND, not detected; NS, not significant; NA, not applicable; Not det., not determined.

abundance could be deduced from the two-dimensional gels (Figure 2), a few selected proteins are described in more detail here. Consistent with the major function of leaf peroxisomes in glycolate recycling, the most prominent protein spots on the two-dimensional gels represented the enzymes involved in the photorespiratory C_2 cycle, all of which were identified (see Supplemental Table 1 online). On the basis of the MS data (see Supplemental Table 2 online), closely related isoforms of high sequence similarity could often be distinguished, allowing conclusions on isoform expression and predominance in mature leaves. For instance, both isoforms of glycolate oxidase (GOX), GOX1 (At3g14415; PRL>) and GOX2 (At3g14420; ARL>), were specifically identified. Of the two isoforms each of Glu-glyoxylate aminotransferase (GGT) and peroxisomal malate dehydrogenase (pMDH), GGT1 (At1g23310; SKM>) and pMDH2 (At5g09660; RIx_5HL) dominated over the second isoform, both of which were identified as well and are thus not restricted to nonphotosynthetic tissue (see Supplemental Tables 1 and 2 online). Catalase isoform 3 (CAT3; At1g20620; 80% identical with CAT1 and 2) was more prominent on the two-dimensional gel than CAT2 (At4g35090), even though these isoforms could hardly be separated by isoelectric focusing. CAT1 (At1g20630) was below the detection limit of the gel-based method but was identified by the shotgun method. Three further antioxidative enzymes were identified as well (see Supplemental Table 1 online).

Even though fatty acid β-oxidation is primarily performed by glyoxysomes of germinating seeds and is thought to play only a minor role in leaves, we detected not only a complete set of the core β-oxidation enzymes but also several auxiliary enzymes in leaf peroxisomes. The core β-oxidation enzymes included long-chain acyl-CoA synthetase isoform 7 (LACS7; At5g27600; SKL>); acyl-CoA oxidase isoform 4 (ACX4; At3g51840; SRL>); both *Arabidopsis* isoforms of multifunctional protein (i.e., multifunctional protein isoform 2 [MFP2; At3g06860; SRL>]) and abnormal fluorescence meristem 1 (AIM1; At4g29010; SKL>); and all three thiolase isoforms. Peroxisome Defective 1 (PED1/KAT2; At2g33150; RQx_5HL) and peroxisomal keto-thiolase isoform 2 (PKT2/KAT5; At5g48880; RQx_5HL) predominated on two-dimensional gels, whereas PKT1/KAT1 (At1g04710; RQx_5HL) was identified only by the shotgun approach.

The auxiliary enzymes of fatty acid β-oxidation included $\Delta^{3,5}$-$\Delta^{2,4}$- dienoyl-CoA isomerase (DCI; At5g43280; AKL>; Goepfert et al., 2005), enoyl-CoA hydratase isoform 2 (ECH2; At1g76150; Goepfert et al., 2006), sterol carrier protein isoform 2 (SCP-2; At5g42890; SKL>; Edqvist et al., 2004), and acyl-CoA thioesterase (ACH2; At1g01710; SKL>; Tilton et al., 2004). With respect to hormone biosynthesis, not only OPR3 but also 3-oxo-2-(2′-pentenyl)-cyclopentane-1-octanoic acid (OPC-8:0) CoA ligase 1 (OPCL1; At1g20510; SKL>), which activates OPC-8:0 (Koo et al., 2006), was detected. OPCL1 was represented by a

low-abundance protein spot restricted to peroxisomes of highest purity, consistent with its low expression level under standard conditions and its induction by wounding. Two further acyl-CoA acitivating enzymes (AAEs) included AAE7/ACN1 (At3g16910; SRL>; Turner et al., 2005) and 4-coumarate-CoA ligase-like protein 1 (4CLP1; At4g05160; SKM>; Schneider et al., 2005). In agreement with the heat inducibility of one of the two sHsps from plant peroxisomes (HSP15.7-Px; Ma et al., 2006), only the constitutively expressed isoform ACD31.2-Px (At1g06460; RLx_5HF) was identified. As peroxisomal membranes were not further enriched prior to proteome analysis, the number of integral membrane proteins identified was low (APX3, PEX11d, and PEX14), which is consistent with the low content of membrane proteins in peroxisomes in general (Fujiki et al., 1982; S. Reumann, unpublished data).

In summary, the 36 known plant peroxisomal proteins identified in isolated leaf peroxisomes included all soluble enzymes involved in photorespiration, ROS metabolism, and JA biosynthesis. The detection of many core and auxiliary enzymes involved in fatty acid β-oxidation and sulfur and nitrogen metabolism (see Supplemental Table 1 online) indicated that (1) the dynamic range of protein identification was sufficiently high to cover low-abundance enzymes that are predominantly expressed in peroxisome variants other than leaf peroxisomes and that (2) β-oxidation–related enzymes may play a yet underestimated role in leaf peroxisomal metabolism.

Several matrix enzymes, although encoded by single *Arabidopsis* genes, often appeared on the two-dimensional gels as multiple protein spots arranged in a characteristic horizontal pattern. This pattern was most obvious for highly abundant matrix enzymes, namely GGT1, Ser-glyoxylate aminotransferase, HPR, and pMDH2, but also observed for minor enzymes, such as ascorbate peroxidase (APX3) and OPCL1 (Figure 2; see Supplemental Figures 2A to 2C online). The horizontal spot series of CAT3 differed slightly in that the differences in pI between spots were smaller (see Supplemental Figure 2D online). Although horizontal spot trains are often seen as artifacts of 2-DE, the uniform and regular patterns observed here might be indicative of the presence of charge-modifying posttranslational modifications, such as phosphorylation and acetylation.

Novel Plant Peroxisomal Proteins

Among the 42 novel proteins, a surprisingly large number had annotated functions related to fatty acid β-oxidation (Table 2). One protein is a yet uncharacterized isoform of the extended superfamily of acyl-activating enzymes, namely AAE5 (At5g16370; SRM>), belonging to clade VI of largely unknown PTS1-carrying AAEs, as does AAE7/ACN1 (Shockey et al., 2003; Reumann et al., 2004; Turner et al., 2005). Regarding the superfamily of enoyl-CoA hydratases/isomerases (ECHIs; Reumann et al., 2004), with MFP and AIM1 being the most prominent enzymes, we now identified monofunctional members of plant peroxisomes. The first ECHI, referred to as isoform a (ECHIa; At4g16210; SKL>), belongs to clade VI of putative plant enoyl-CoA hydratases. Two further monofunctional ECHIs identified, namely, ECHIb (At4g14430; PKL>) and ECHIc (At1g65520; SKL>), have been grouped in clade III and are the closest *Arabidopsis* homologs of peroxisomal monofunctional Δ^3-Δ^2-enoyl-CoA isomerase (PECI) from fungi and mammals (Geisbrecht et al., 1999; Reumann et al., 2004). Most intriguing of this enzyme family is ECHId, annotated as putative naphthoate synthase (NS/ECHId; At1g60550; RLx_5HL) because the enzyme is plant specific among eukaryotes and represents the *Arabidopsis* homolog of cyanobacterial MenB (clade V), an enoyl-CoA hydratase involved in phylloquinone biosynthesis (Johnson et al., 2001; Gross et al., 2006, see also references therein). This provides experimental evidence for peroxisome targeting of the single *Arabidopsis* homolog of MenB, further supported by conservation of the predicted PTS2 in homologous ESTs (see Supplemental Figure 3O online), and indicates that phylloquinone biosynthesis is partly compartmentalized in plant peroxisomes.

One protein spot was identified as a monofunctional hydroxyacyl-CoA dehydrogenase, annotated as hydroxybutyryl-CoA dehydrogenase (HBCDH; At3g15290) and carrying the predicted major PTS tripeptide PRL> (Reumann et al., 2004). Of the experimentally uncharacterized *Arabidopsis* family of small thioesterases (STs) with six PTS1-possessing members (Reumann et al., 2004), the second isoform of clade I (ST2; At1g04290; SNL>) is now experimentally associated with plant peroxisomes. Five novel proteins belong to the superfamily of short (polypeptide)-chain dehydrogenases/reductases (SDRs) and include four monofunctional SDRs (SDRa, At4g05530, SRL>; SDRb, At3g12800, SKL>; SDRc, At3g01980, SYM>; and SDRd, At3g55290, SSL>) and a bifunctional short- and medium-chain dehydrogenase/reductase (BSMDR; At1g49670; SRL>) with an N-terminal SDR and a C-terminal medium-chain dehydrogenase/reductase domain of the subgroup of NADPH:quinone reductases (COG0604, Qor). The latter was identified specifically by the gel-free approach.

Further novel enzymes with predicted catalytic activities related to fatty acid β-oxidation included epoxide hydrolase isoform 3 (EH3; At4g02340; ASL>) and one of two *Arabidopsis* homologs of acetoacetyl-CoA thiolase (ACAT2, EC 2.3.1.9, At5g48230, which is 80% identical with ACAT1, At5g47720; Carrie et al., 2007). GOX3 (At4g18360; AKL>) is a yet unknown isoform that shares 85% identity at the amino acid level with GOX1/2 but is predominantly expressed in nonphotosynthetic tissue and presumably plays a role outside of photorespiration (Kamada et al., 2003; Reumann et al., 2004). Enzymes associated with peroxisomal NADP metabolism included isoforms of NADP-dependent isocitrate dehydrogenase (IDH; At1g54340; SRL>) and 6-phosphogluconate dehydrogenase (6PGDH; At3g02360; SKI>), one of three enzymes of the oxidative pentose phosphate pathway (OPPP). Several novel plant peroxisomal enzymes are predicted to catalyze GSH-dependent reactions. These identified proteins included an isoform of glutathione reductase (GR; At3g24170; TNL>), isoform θ 1 of the extended *Arabidopsis* family of glutathione *S*-transferases (GSTT1, formerly GST10, At5g41210, SKI>, EC 2.5.1.18; Dixon et al., 2002), and the single *Arabidopsis* homolog of *S*-(hydroxymethyl)glutathione dehydrogenase (HMGDH; At5g43940; EC 1.1.1.284; Dolferus et al., 1997).

Seven identified proteins are functionally associated with plant defense mechanisms, which was rather unexpected. Four enzymes are β-glucosidases of the superfamily of glycoside

hydrolase family 1, many of which are reported to mediate plant defense against herbivores (Xu et al., 2004; Table 2). The β-glucosidases included β-glucosidase 1 (BGL1; At1g52400; Stotz et al., 2000), PYK10 (At3g09260), and the myrosinase homolog thioglucoside glucohydrolase 2 (TGG2; At5g25980; Barth and Jander, 2006). All three defense-related enzymes were apparently upregulated in leaf peroxisomes isolated from senescent plants (see Supplemental Figures 2E and 2F online); TGG1 (At5g26000; Barth and Jander, 2006) was specifically identified in the latter (data not shown). The myrosinase-associated protein EPITHIOSPECIFIER MODIFIER1 (ESM1; At3g14210), which alters glucosinolate hydrolysis and insect resistance (Zhang et al., 2006), was identified in highly purified leaf peroxisomes as well. Two other defense proteins identified comprised one of three *Arabidopsis* homologs of vertebrate macrophage migration inhibitory factor (MIF; At3g51660; SKL>) and ozone-induced protein 1 (OZI1; At4g00860), a plant-specific small polypeptide of only 80 residues that is induced by ozone and pathogen attack (Sharma and Davis, 1995).

Likewise unexpected was the identification of proteins with annotated functions related to nucleic acid metabolism. These six proteins included two Gly-rich RNA binding proteins (GRP7 and 8; At2g21660 and At4g39260; Staiger et al., 2003), two DEAD-box RNA helicases (RH11, At3g58510; RH37, At2g42520), an unknown RNA binding protein (RBP; At4g17520), and a nucleotide binding protein (NBP; At4g16566). Except for NBP carrying the PTS1-like C-terminal tripeptide SKV>, all proteins related to nucleic acid metabolism lack predicted PTSs.

Proteins with other annotated functions included two enzymes reported to be involved in Cys and Met biosynthesis. *O*-acetylserine sulfhydrylase (OASS A1; At4g14880) is a presumably cytosolic isoform lacking an obvious PTS. Isoform 1 of cobalamin (vitamin B12)-independent Met synthase (METE1; At5g17920; EC 2.1.1.14; Ravanel et al., 2004) carries the PTS1-related C-terminal tripeptide SAK>. One of two *Arabidopsis* homologs of betaine aldehyde dehydrogenase (BADH; At3g48170; SKL>) was identified as well, homologs of which had previously been localized to the peroxisome matrix in monocotyledons (Nakamura et al., 1997). Another protein spot (ATF1; At1g21770; SSI>) was identified as a closely related homolog of a recently crystallized minimal acetyl transferase (ATF2; At1g77540; SSI>; Tyler et al., 2006). The single *Arabidopsis* transthyretin-like protein (TLP; At5g58220) is homologous to mammalian transthyretin, a transport protein for vertebrate hormones (Eneqvist et al., 2003; Hennebry et al., 2006a, 2006b). Interestingly, the full-length protein contains a predicted PTS2 (RLx_5HL) outside of the N-terminal domain in a linker region that connects two enzymatic domains, whereas two alternative splice variants from *Arabidopsis* lack the putative targeting signal (Figure 3A; see Supplemental Figure 3P online; Hennebry et al., 2006a; Ramazzina et al., 2006). By MS sequencing of three tryptic peptides covering major parts of the linker region, including the putative PTS2, the TLP homolog identified in *Arabidopsis* peroxisomes was demonstrated to represent the full-length protein, strengthening the idea that the internal PTS2 peptide targets full-length TLP to peroxisomes (Figure 3). Lastly, four novel proteins lacked annotated domains and sequence similarity with known proteins deposited in the protein databases; three of these unknown proteins (UPs) carried PTS-like tripeptides (UP1, At1g52410, SSL>; UP2, At3g15950, SLN>; and UP3, At2g31670, SSL>; Table 2).

In Silico Analysis of the Targeting Function of Putative PTS Peptides

The majority of the novel proteins found to be associated with leaf peroxisomes (64%) carried predicted well-known PTSs (16 proteins; Reumann, 2004) or PTS-related peptides, for instance, SSL>, SSI>, ASL>, SAK>, or SYM> (11 proteins; Table 2), strongly supporting their localization in the peroxisome matrix. Because the sole presence of a putative PTS peptide is an insufficient criterion to definitely conclude peroxisome targeting (see Introduction), we further investigated the predicted targeting function of PTS peptides using both computational and experimental analyses. As part of the computational analyses, predicted orthologs of the novel proteins were retrieved from protein and EST databases of higher plants and analyzed for conservation of the predicted targeting peptides as outlined previously (Reumann, 2004; Reumann et al., 2004). Most proteins fulfilled the initial requirements for subsequent analysis except for a few proteins that either appeared to be specific to *Brassicaceae* (e.g., EH3 and UP1-3) or shared high sequence similarity with other *Arabidopsis* homologs (e.g., SDRd, BADH, GOX3, and METE1), preventing the specific detection of apparent orthologs.

On average, 30 plant ESTs were retrieved for each novel protein. Except for one EST homologous to SDRa terminating with FRL>, the orthologs of nine novel proteins with predicted PTS1 (ECHIa/b/c, ST2, SDRa/c, BSMDR, GSTT1, and MIF) carried approximately four different C-terminal tripeptides each, all of which represented major or minor PTS1s (see Supplemental Figure 3 online). Five other novel proteins had previously been reported to carry conserved PTS1 (SDRb/DECR, HBCDH, IDH, 6PGL, and 6PGDH; Reumann et al., 2004). Likewise, the postulated peroxisome-targeting function of the PTS1-related tripeptide SSI> present in ATF1 was supported by the detection of several homologous ESTs possessing either minor noncanonical PTS1s (SSM> or SNM>) or closely related tripeptides, such as SHI> and SNI> (see Supplemental Figure 3N online). In addition, most plant homologs of ATF1 carried a basic residue at position −4, which is reported to enhance peroxisome targeting by weak PTS1 tripeptides (Mullen et al., 1997; Maynard et al., 2004). Regarding SDRc (SYM>), only PTS1-like peptides were present in homologous ESTs (e.g., SF[ML]>, AYM>; see Supplemental Figure 3H online). However, the high content of basic amino acid residues and Pro in front and the lack of acidic residues in the C-terminal tripeptides themselves were consistent with protein targeting by the PTS1 pathway. Although a dissection of plant homologs of ACAT2 into apparent orthologs of ACAT1 or ACAT2 was difficult, many EST sequences were found to carry C-terminal 10–amino acid extensions either terminating with predicted (SKL>) or novel PTS1s (SSL>; see below) or PTS1-like tripeptides (SAL> or SLL>; see Supplemental Figure 3J online).

Regarding novel proteins carrying predicted PTS2, the peroxisome targeting function of the predicted PTS2 in naphthoate synthase (NS/ECHId; At1g60550; RLx_5HL) was well supported by conservation of the nonapeptide as major or minor PTS2 ($R[LIMV]x_5HL$) in plant orthologs. Moreover, characteristic amino

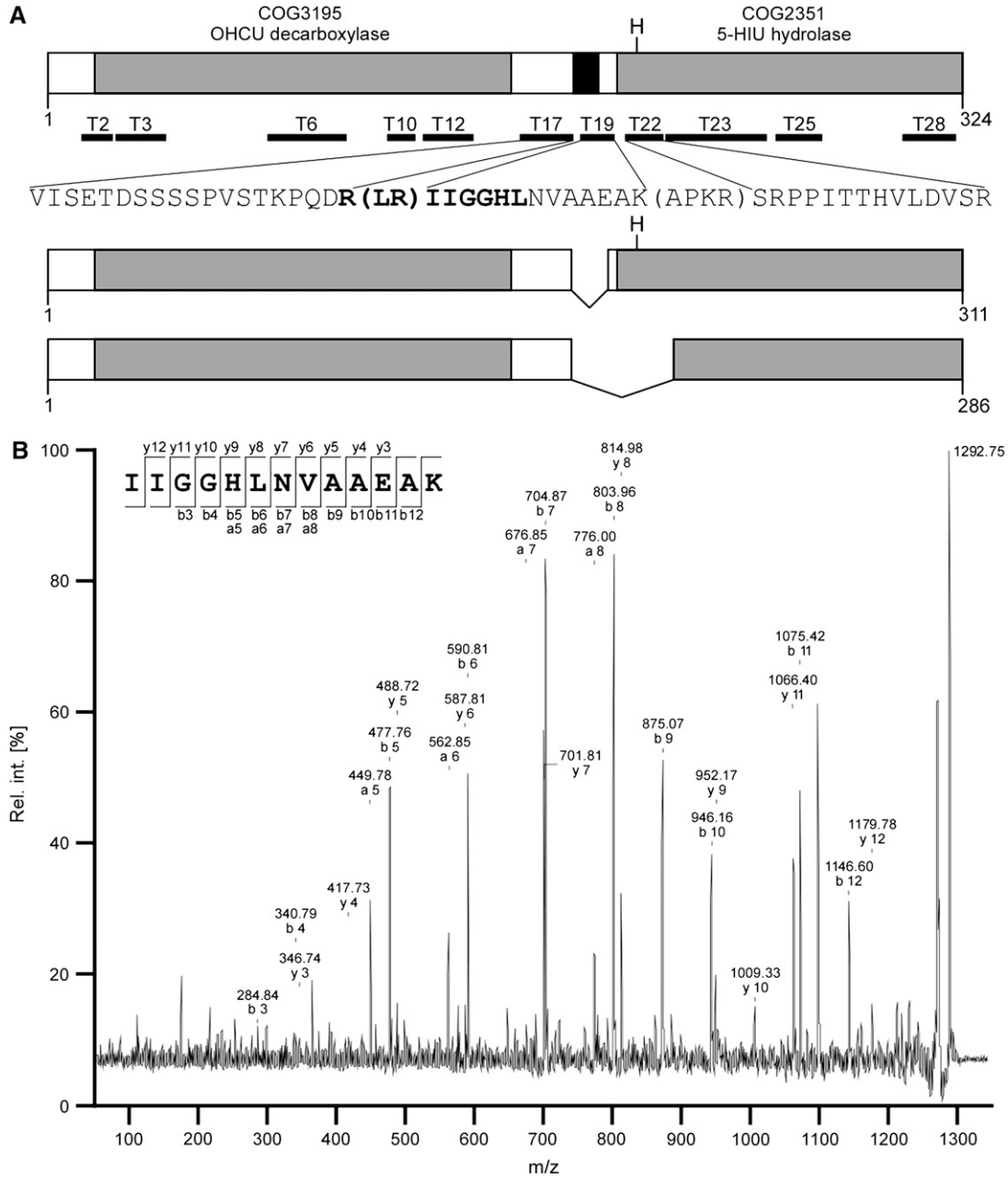

Figure 3. Domain Structure of *Arabidopsis* Transthyretin-Like Protein and Its Splice Variants.

The single *Arabidopsis* TLP (At5g58220) is a bifunctional protein with an N-terminal decarboxylase (COG3195, OHCU decarboxylase) and a C-terminal hydrolase domain (COG2351, 5-HIU hydrolase) synthesized in three splice variants **(A)**. The full-length variant (TLP_{324}) carries a predicted PTS2 (RLRIIGGHL, position 182 to 190) in the linker region between the two functional domains. In addition to the peptide mass information obtained (shown in **[A]** as black bars with numbering of tryptic peptides), mass spectrometric sequencing by MALDI-TOF-MS unambiguously confirmed the presence of the tryptic peptides T17, T19, and T22 (shown in **[A]** also as sequences, PTS2 amino acids in bold face), thereby indicating the integrity of the linker region of full-length TLP_{324}. Except for the tryptic dipeptide T18 (LR) that escaped detection due to its small size, the entire PTS2 nonapeptide was covered by the sequencing analysis, as can be deduced from the fragment ion mass spectrum of T19 **(B)**. By contrast, both shorter splice variants of TLP (TLP_{311} and TLP_{286}) lack the internal PTS2 and TLP_{286} additionally the bulky conserved His residue (His_{209} of TLP_{324}, corresponding to His_{14} of TLP/PucM of *Bacillus subtilis*) that is implicated in determining the entrance diameter of the internal channel (Jung et al., 2006). Thus, the shorter transcriptional variants probably differ in subcellular localization and function from the peroxisomal isoform. See Supplemental Figure 3P online for details of the central amino acid sequence of the three *Arabidopsis* TLP splice variants and plant homologs. OHCU, 2-oxo-4-hydroxy-4-carboxy-5-ureidoimidazoline.

acid residues predicted to act as targeting-enhancing elements (Arg and Pro) were present in close proximity to the PTS2 (Reumann, 2004; see Supplemental Figure 3O online). Likewise, the predicted internal PTS2 (RLx_5HL) of TLP was conserved as putative major or minor PTS2s in all homologous plant ESTs spanning this region (e.g., $R[LIMV]x_5HL$ and RIx_5HM) except for one slightly divergent nonapeptide (RVx_5HV) present in *Medicago* (see Supplemental Figure 3P online). Even though full-length TLP variants appear to predominate among plant ESTs, some plant species, such as *Oryza* and *Triticum*, were found to express alternative splice variants similar to *Arabidopsis* that exactly lack this nonapeptide (Figure 3B; see Supplemental Figure 3P online; Hennebry et al., 2006a).

Experimental Verification of Predicted PTSs

To experimentally verify protein targeting to peroxisomes and the peroxisome-targeting function of predicted PTSs, subcellular targeting of seven representative fusion proteins with EYFP was analyzed by fluorescence microscopy upon transient cDNA expression in onion epidermal cells. Four proteins carried predicted major PTS1 peptides (SRL>, SKL>, or PRL>), whereas three proteins possessed predicted minor PTS1s (SKI> or PKL>) of lower peroxisome-targeting probability (Reumann, 2004). For all proteins, subcellular targeting of two constructs was analyzed (i.e., EYFP fusions of the full-length proteins of interest and fusions attaching only the predicted PTS1 targeting domain [PTD], comprising the C-terminal 10–amino acid residues, including the putative PTS1 tripeptide, to EYFP).

NADP-dependent IDH (At1g54340; SRL>) was chosen as one of the proteins carrying predicted major PTS1 peptides. NADP-dependent IDH, fused at its N terminus with EYFP (EYFP-IDH), was indeed detected in punctate structures in onion epidermal cells (Figure 4A1). In double transformants expressing simultaneously a peroxisome-targeted cyan fluorescent protein (CspMDH-CFP; Fulda et al., 2002; Ma et al., 2006), the yellow fluorescent subcellular structures were identified conclusively as peroxisomes (Figures 4A1 and 4A2). EYFP extended by the C-terminal 10–amino acid residues of IDH, including the predicted PTS1 SRL> ($EYFP\text{-}PTD_{IDH}$), was directed from the cytosol to punctate structures, thereby identifying SRL> as the PTS of peroxisomal IDH (Figure 4B). Two further proteins, namely, the full-length fusion proteins of the predicted DECR homolog SDRb (At3g12800; SKL>) and the monofunctional hydroxyacyl-CoA dehydrogenase HBCDH (At3g15290; PRL>), were targeted to peroxisomes as well (Figures 4C1, 4C2, 4E1, and 4E2). EYFP extended by the PTDs of these proteins showed a punctate fluorescence pattern, characterizing the C-terminal tripeptides SKL> and PRL> as the targeting signals of SDRb/DECR and HBCDH, respectively (Figures 4D and 4F).

Regarding proteins carrying predicted minor PTS1 peptides, the fusion protein between EYFP and ECHIb (At4g14430; PKL>), one of two predicted homologs of mammalian PECI (Geisbrecht et al., 1999), was targeted to punctate structures in onion epidermal cells that coincided with CFP-labeled peroxisomes (Figures 4I1 and 4I2). EYFP, extended by the C-terminal 10–amino acid residues of ECHIb, including the predicted PTS1 PKL> ($EYFP\text{-}PTD_{ECHIb}$), was directed from the cytosol to punctate structures, thereby identifying the minor PTS1 PKL> as the PTS of peroxisomal ECHIb (Figure 4J). Likewise, the isoform GSTT1 (At5g41210) with the putative PTS1 SKI> was shown to be located in peroxisomes, as the yellow fluorescent spots coincided with cyan fluorescent peroxisomes upon expression of *EYFP-GSTT1* (Figures 4K1 and 4K2). The transferase was imported into peroxisomes via the PTS1 pathway because attachment of the C-terminal 10–amino acid domain of GSTT1 to EYFP showed a punctate pattern of fluorescence (Figure 4L). The full-length protein of the NADPH-producing dehydrogenase 6PGDH (At3g02360; SKI>) fused to the C-terminal end of EYFP was the only full-length fusion protein that remained cytosolic, for yet unknown reasons (Figure 4M). The C-terminal 10–amino acid residues of 6PGDH, however, directed EYFP to punctate subcellular structures that moved along cytoplasmic strands and coincided with peroxisomes (Figures 4N1 and 4N2). Although not identified within the proteome analysis, subcellular targeting of 6P-gluconolactonase (6PGL), the precedent enzyme of 6PGDH in the peroxisomal OPPP (Corpas et al., 1998, 1999), was also investigated using one specific isoform (At5g24400) out of five *Arabidopsis* homologs. This enzyme carries both a predicted N-terminal transit peptide and a conserved PTS1 (SKL>; Reumann et al., 2004). Whereas 6PGL-EYFP was targeted to plastid-like structures consistent with the presence of a functional N-terminal transit peptide (see Supplemental Figure 4 online), the inversely arranged fusion protein, EYFP-6PGL, was targeted to peroxisomes (Figures 4G1 and 4G2), as was $EYFP\text{-}PTD_{6PGL}$ with the PTS1 SKL> (Figure 4H). These data further strengthen the idea that this 6PGL isoform is targeted to both plastids and peroxisomes in vivo, probably regulated by alternative translation (Reumann et al., 2004).

Taken together, predicted peroxisome targeting of novel proteins identified in isolated leaf peroxisomes was experimentally confirmed for five of the six full-length candidate proteins and additionally for 6PGL as a metabolically related enzyme; all predicted PTS1s were characterized as the functional targeting signals of the respective proteins. Peroxisome targeting of full-length 6PGDH may have been disturbed by the N-terminal EYFP tag or depend on yet unknown auxiliary import factors missing in the standard expression system of onion epidermal cells.

Characterization of Novel Targeting Peptides

We next investigated whether representative novel proteins carrying PTS1-related peptides at the extreme C terminus or PTS2 peptides outside of the defined N-terminal domain are indeed imported into peroxisomes and whether these peptides function as targeting signals. The three PTS1-related tripeptides chosen for these experiments were SSL>, SSI>, and ASL>. The full-length fusion protein composed of EYFP and *Arabidopsis* enoyl-CoA hydratase ECH2 (At1g76150; SSL>) was targeted to peroxisomes (Figures 5A1 and 5A2). Extension of EYFP by the C-terminal 10–amino acid residues of ECH2 directed the reporter protein to punctate structures that coincided with peroxisomes (Figures 5B1 and 5B2); thus, the C-terminal PTS1-like tripeptide SSL> is the PTS1 of ECH2 and a novel functional PTS1 tripeptide in higher plants. Likewise, EYFP-ATF1 (At1g21770) terminating with SSI> was detected in peroxisomes (Figures 5C1 and 5C2).

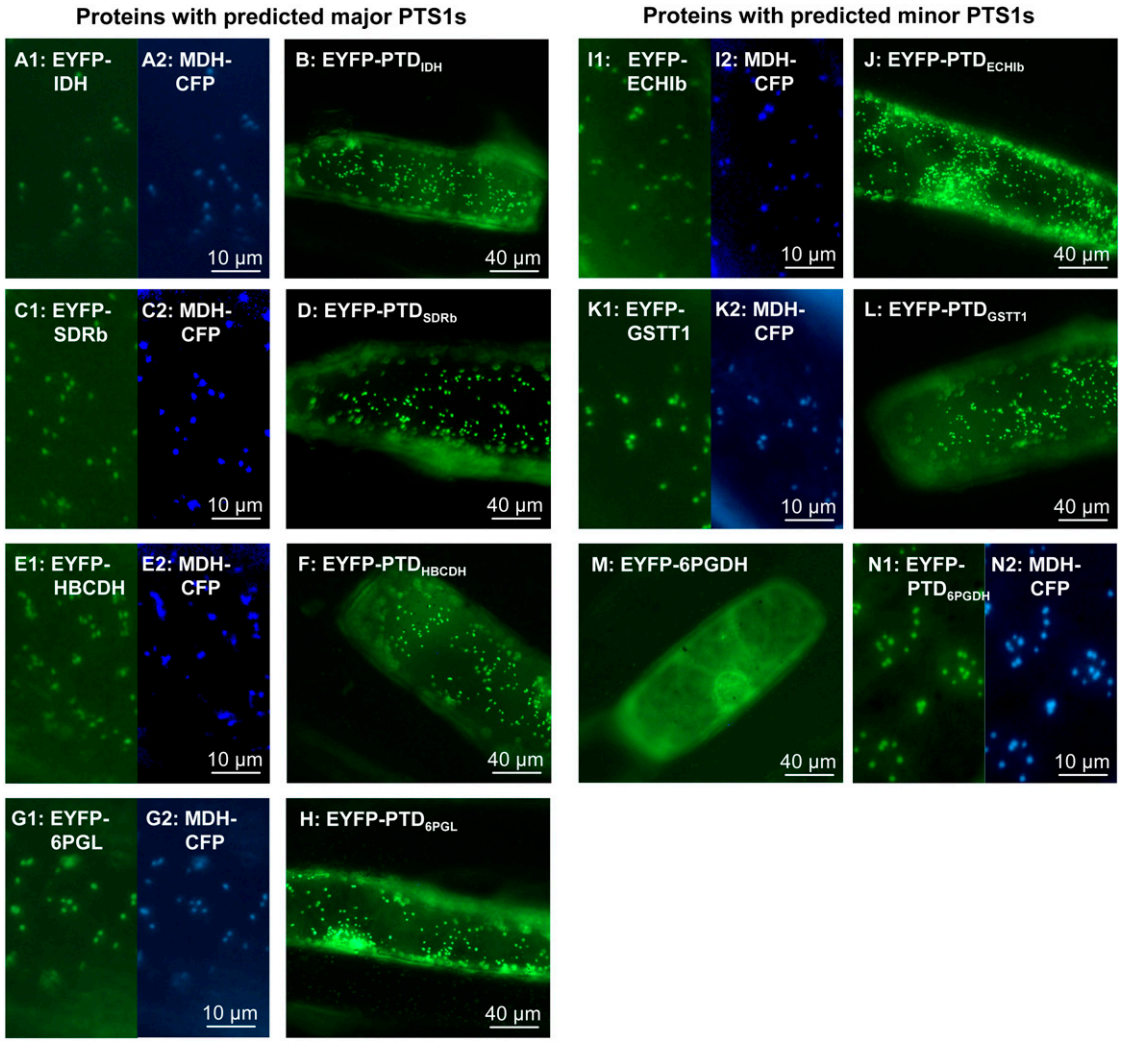

Figure 4. Verification of Peroxisome Targeting of Novel Peroxisomal Proteins Carrying Predicted Major or Minor PTS1s.

The cDNAs of six novel peroxisomal proteins identified in isolated leaf peroxisomes from *Arabidopsis* and one pathway-associated protein (6PGL) were fused in frame to the 3′ end of EYFP and transiently expressed in onion epidermal cells upon cell bombardment. Fluorescence microscopy was used to determine whether fusion proteins were targeted to punctate subcellular structures that coincided with peroxisomes labeled with a peroxisome-targeted version of CFP, MDH-CFP (Fulda et al., 2002). In addition, we analyzed the targeting of EYFP extended C-terminally by the putative 10–amino acid residue PTDs of the respective proteins. 6PGL was not yet identified in isolated leaf peroxisomes but analyzed in context of the detection of another peroxisomal isoform of the OPPP, 6PGDH. The following proteins were found to be targeted to peroxisomes by functional PTS1s (see text for full names): IDH (At1g54340, SRL>; A1, A2, 95% overlapping dots; **[B]**), SDRb (At3g12800, SKL>; **[C1]** and **[C2]**; 74% overlapping dots; **[D]**), HBCDH (At3g15290, PRL>; **[E1]** and **[E2]**; quantification difficult; **[F]**), 6PGL (At5g24400, SKL>; **[G1]** and **[G2]**; 95% overlapping dots; **[H]**), ECHIb (At4g14430, PKL>; **[I1]** and **[I2]**; 97% overlapping dots; **[J]**), and GSTT1 (At5g41210, SKI>; **[K1]** and **[K2]**; 95% overlapping dots **[L]**). The full-length fusion protein of 6PGDH (At3g02360) remained cytosolic **(M)**, although it was shown to contain a functional PTS1 (SKI>; **[N1]** and **[N2]**; 91% overlapping dots).

The putative PTS1 domain of this protein directed EYFP to punctate structures that coincided with peroxisomes, establishing SSI> as a second novel plant PTS1 (Figures 5D1 and 5D2). For epoxide hydrolase isoform 3 (EH3; At4g02340) carrying the C-terminal PTS1-like tripeptide ASL>, organelle targeting was difficult to demonstrate owing to a pronounced cytosolic background staining. Nevertheless, protein targeting to peroxisomes could be demonstrated by double labeling in a few cells (Figures 5E1 and 5E2). Attachment of the C-terminal 10–amino acid residues of EH3 to EYFP directed the reporter protein from the cytosol to punctate structures that coincided with peroxisomes (Figured 5F1 and 5F2). With these results, we conclusively demonstrated targeting of another three proteins to peroxisomes (ECH2, ATF1, and EH3) and established the PTS1-like peptides SSL>, SSI>, and ASL> as novel functional PTS1 peptides for higher plants.

By current definition, PTS2 nonapeptides are confined to the N-terminal domain comprising ~40 amino acid residues. To

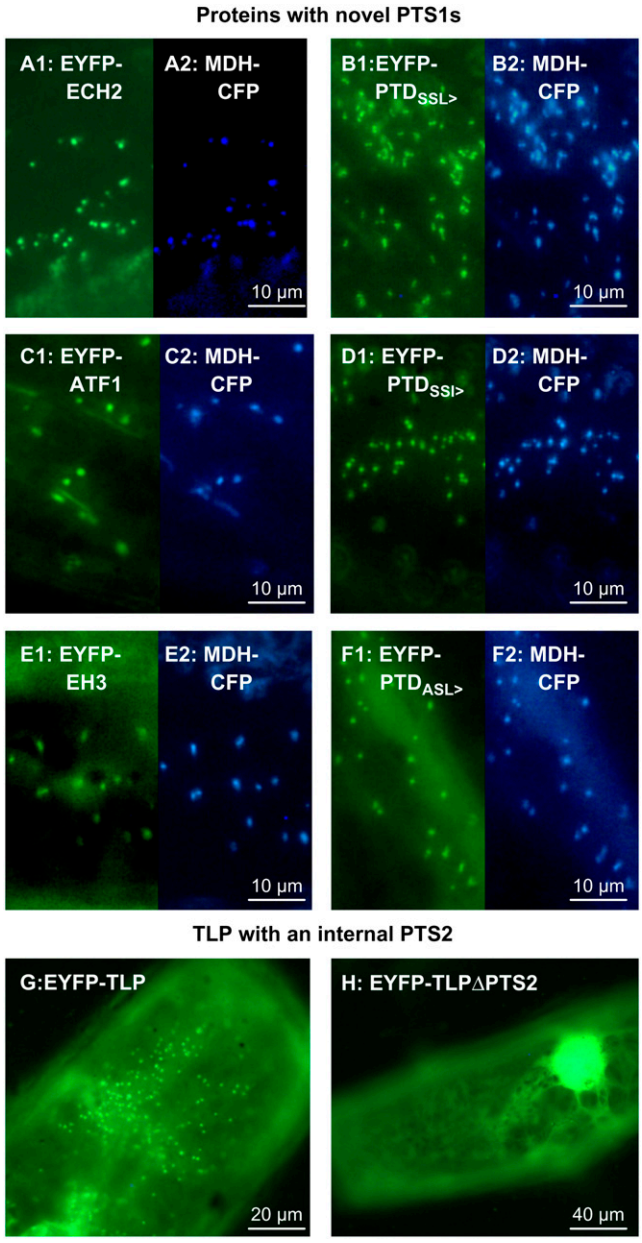

Figure 5. Subcellular Targeting Analysis of Novel Peroxisomal Proteins Carrying Unknown PTSs.

The generation of EYFP fusion proteins and the fluorescence microscopic analyses were performed as described in Figure 4. Subcellular targeting analysis of ECH2 (At1g76150, SSL>; **[A1]** to **[B2]**; **[A]**, 71% overlapping dots; **[B]**, 95% overlapping dots), ATF1 (At1g21770, SSI>; **[C1]** to **[D2]**; **[C]**, 60% overlapping dots; **[D]**, 59% overlapping dots), and EH3 (At4g02340, ASL>; **[E1]** to **[F2]**; **[E]**, 80% overlapping dots; **[F]**, 73% overlapping dots) established SSL>, SSI>, and ASL> as novel functional PTS1 peptides in plants. Although analysis of full-length TLP_{324} (At5g58220) carrying a putative internal PTS2 (RLx_5HL) at least indicated targeting to punctate subcellular structures **(G)**, we could not provide conclusive evidence for peroxisomal localization of EYFP-TLP_{324} by double labeling owing to a strong cytosolic background fluorescence. When the essential His of the predicted internal PTS2 was mutated to Asp (RLx_5HL to RLx_5DL) to generate EYFP-TLPΔPTS2, the punctate fluorescence pattern disappeared **(H)**, enabling us to identify the full-length version of TLP_{324}, but not the two shortened splice variants lacking the predicted PTS2 (TLP_{311} and TLP_{286}; see Figure 3) as a peroxisomal protein that is targeted to the organelle by an internal PTS2.

determine whether the bifunctional TLP identified in *Arabidopsis* leaf peroxisomes (Figures 2 and 3, Table 2) was targeted to peroxisomes by the internally located putative PTS2 (RLx_5HL), the full-length cDNA of TLP was cloned downstream of *EYFP* and transiently expressed in onion epidermal cells. The fusion protein EYFP-TLP was detected mainly in the cytosol. However, despite the strong background fluorescence, targeting of EYFP-TLP to punctate structures suggestive of peroxisomes was observed in some cells (Figure 5G). The low contrast between the yellow fluorescent punctate structures and the background, however, allowed conclusive organelle identification as peroxisomes by double labeling only in a single cell (data not shown). In an alternative approach, the His residue known to be essential for the targeting function of PTS2 (Kato et al., 1998; Reumann, 2004; Ma et al., 2006) was mutated to Asp ($RLx_5HL \rightarrow RLx_5DL$). Indeed, the mutated fusion protein EYFP-TLPΔPTS2 was no longer targeted to peroxisomes but exclusively detected in the cytosol and the nucleus, as was EYFP alone (Figure 5H). Thus, these data demonstrate targeting of a eukaryotic TLP homolog to peroxisomes and an internal location of a functional PTS2 in an endogenous eukaryotic protein.

Analysis of Artificial Copurification of Large Protein Complexes with Leaf Peroxisomes

The defense- and nucleic acid metabolism-related proteins identified in isolated leaf peroxisomes were represented by a relatively high number of proteins lacking known PTSs. Some of these defense-related proteins, such as BGL1, PYK10, and *Brassica* myrosinases, are reported to form polymers (Eriksson et al., 2002; Nagano et al., 2005; Lee et al., 2006). Likewise, nucleic acid metabolism-related proteins may be components of large protein complexes, such as ribosomes, exosomes, spliceosomes, or P-bodies (for review, see Eulalio et al., 2007). Even though unlikely, it was conceivable that these proteins were accidentally copurified with leaf peroxisomes through large complexes of similar sedimentation behavior in density gradient centrifugation. To distinguish between a physiologically relevant or artificial association of defense- and nucleic acid metabolism-related proteins with leaf peroxisomes, the isolation protocol was modified in such a way that intact leaf peroxisomes were lysed in hypoosmotic media by conditions that are not expected to reduce the sedimentation rate of protein complexes. To this end, *Arabidopsis* leaves were worked up in grinding and washing buffer lacking sucrose under otherwise identical conditions. Indeed, the fractions of the sucrose density gradient corresponding to those of intact leaf peroxisomes (fractions 11 and 12, Figure 1) contained substantially less total protein and largely lacked HPR activity, indicating that intact leaf peroxisomes were efficiently lysed and no longer recovered (data not shown). When

Table 3. Proteins Identified in *Arabidopsis* Leaf Peroxisomes

	Known Proteins			Novel Proteins					Predicted Proteins	
	Total	Matrix	Membrane	Total	PTS1	PTS2	PTS-Like	Non-PTS1	PTS1	PTS2
Up to 2007	75	51	24	–	–	–		–	221	60
This study	36	33	3	43	21	2	5	15	311	61[1]

Of the 51 known matrix proteins reported up to 2007 to be targeted to plant peroxisomes, 33 (65%) were identified in this proteome study of *Arabidopsis* leaf peroxisomes. With respect to membrane proteins, the coverage of known proteins is significantly reduced (3 out of 24), consistent with the low content of membrane proteins in the entire proteome of the organelle. In total, 43 novel peroxisomal proteins were identified (42 by the proteome approach, 6PGL as EYFP fusion protein). Approximately half of the novel proteins (21; 49%) carry a previously defined PTS1 tripeptide (16 proteins; Reumann, 2004) or one of three novel functional PTS1 tripeptides (SSL>, SSI>, and ASL>) identified in this study (five proteins). The identification of three novel PTS1 tripeptides increases the number of putative PTS1 proteins encoded in the *Arabidopsis* genome by 40%, from 221 to 311. Even though a considerable number of *Arabidopsis* proteins carry a predicted PTS2 at an internal position, as does TLP ([1], 201 proteins with a major PTS2 and 443 proteins with a minor PTS2), these proteins are not listed because only few bifunctional proteins are expected to expose a functional PTS2 on the protein surface and to represent true positive peroxisomal matrix proteins.

such a fraction volume corresponding to ~200 μg leaf peroxisomal protein in the presence of osmoticum was subjected to 2-DE, none of the defense-related proteins (BGL1, TGG2, PYK10, or ESM1) were detected by Coomassie staining (see Supplemental Figure 5 online). Similarly, the nucleic acid metabolism-related proteins GRP7 and 8 and RBP were not visible. Although two very faint spots may coincide with the RNA helicases RH11 and RH37 (see Supplemental Figure 5 online), these data as a whole strongly argue against an artificial copurification of high molecular weight complexes formed by the defense- or nucleic acid metabolism-related proteins with leaf peroxisomes and support a physiologically relevant association of most if not all of these PTS-deficient proteins with leaf peroxisomes.

DISCUSSION

Only ~50 plant peroxisomal matrix proteins have been established for *Arabidopsis* either experimentally or by homology to peroxisomal proteins from other plant species (see summary at www.araperox.uni-goettingen.de). The low number of known peroxisomal enzymes in general and of plant-specific proteins in particular severely restricts our current knowledge of the organelle's physiological functions and alternative protein targeting mechanisms. The two most promising large-scale approaches to ultimately characterize the proteome of plant peroxisomes in its entity are (1) bioinformatics analyses predicting PTS1 and PTS2 proteins from genome sequences in combination with subcellular targeting studies of candidate fluorescent fusion proteins, and (2) proteome analyses. As in silico predictions are currently limited by several parameters (see Introduction) and because highly pure peroxisomes can finally be isolated from *Arabidopsis*, proteome analysis is the method of choice. This study demonstrates that proteome data yield important information not only directly on the identity of novel proteins and the recognition of newfound metabolic pathways but also indirectly on protein targeting. Leaf peroxisomal proteome analysis enables us to (1) recognize novel targeting peptides, (2) extend the location of PTS2 domains, and (3) posit the existence of novel PTS1/2-independent targeting pathways.

Plant-specific peroxisome functions, such as photosynthesis-related pathways, hormone biosynthesis, and pathogen defense mechanisms, are expected to be most comprehensively depicted by proteome analyses of *Arabidopsis* peroxisomes from mature rosette leaves rather than heterotrophic suspension-cultured cells or germinating seeds, even though these tissues offer significant technical advantages. The challenges in isolating highly pure *Arabidopsis* leaf peroxisomes include not only obvious traits (e.g., low leaf fresh weight and predominance of chloroplasts) but also unexpected parameters, such as the extreme fragility of *Arabidopsis* leaf peroxisomes in aqueous extracts, probably owing to the high concentrations of secondary metabolites, and their pronounced physical association with chloroplasts and mitochondria in *Brassicaceae*. For in-depth proteome analysis, we optimized our previous method (Ma et al., 2006) in several aspects, such as plant growth and time of harvest, differential centrifugation, and by the use of both Percoll and sucrose density gradients in particular (see Results and Methods). Contaminating proteins of chloroplasts and mitochondria, the major contaminants of plant peroxisomes, were hardly detectable in the final fraction by sensitive biochemical methods. The higher apparent content of contaminants estimated from the spot representation on two-dimensional gels (~5%) compared with the activities of compartment-specific marker enzymes (0.1% plastids and 1.7% mitochondria; Table 1) may reflect facilitated solubilization of the rather acidic nonperoxisomal proteins compared with the neutral or basic peroxisomal proteins.

The Proteome Map of *Arabidopsis* Leaf Peroxisomes

The success of organellar proteome studies is determined by the number of novel true positives that indeed reside in the compartment of interest. The gel-based and shotgun approaches applied as complementary protein identification strategies maximized proteome coverage. The 78 proteins identified represent approximately twice as many proteins as reported previously in peroxisomes from rat liver (Kikuchi et al., 2004) or plants (Fukao et al., 2002, 2003). The 33 known matrix proteins include 65% of all currently known matrix proteins from plant peroxisomes (51 *Arabidopsis* proteins; Table 3). As this ratio has been obtained from only one of several plant peroxisomal variants and from standard plants, the coverage is considered high. Comprehensive proteome analyses of other tissue-specific and developmental

peroxisome variants (e.g., glyoxysomes and gerontosomes) and from plants subjected to abiotic or biotic stresses are expected to promote the detection of the remaining known and further predicted proteins. A comprehensive membrane proteome analysis will be made possible by the availability of larger organelle quantities and the selective enrichment of peroxisomal membranes.

Forty-three novel proteins (42 proteins by the proteome approach and 6PGL as an EYFP fusion protein) had not previously been localized to plant peroxisomes in any species and had not, for the most part, been experimentally analyzed. Seventeen of these novel proteins carry previously defined PTSs (16 PTS1 and one PTS2) and had been predicted to be peroxisomal proteins from the *Arabidopsis* genome (Reumann et al., 2004). Together with six predicted PTS1 proteins localized experimentally to peroxisomes in the meantime (4CLP1, AAE7/ACN1, ACH2, DCI, OPCL1, and SCP-2), ~40% of the nonhypothetical *Arabidopsis* proteins (23 out of 50) predicted to be peroxisome targeted with high probability have been covered by our proteome study, confirming reciprocally the in silico approach. The high number of PTS-carrying proteins of this study (30 of 36 known and 22 of 42 novel proteins) contrasts with the low numbers of two previous two-dimensional gel-based peroxisomal proteome studies from greening and etiolated cotyledons (one novel PTS protein out of 20; Fukao et al., 2002; three out of 13; Fukao et al., 2003; see Supplemental Figures 6A and 6B online). With respect to novel protein identity, the overlap between the three proteome studies is marginal (only one protein, i.e., NADP-dependent IDH, At1g54340, SRL>) and difficult to rationalize in light of the large number of β-oxidation–related enzymes reported here for leaf peroxisomes but not previously for glyoxysomes, the peroxisome variant most specialized on fatty acid degradation (Fukao et al., 2003; see Supplemental Figure 6A online). Compared with the methods for peroxisome enrichment (single Percoll gradient only) and protein identification (PMF alone) applied in the two earlier studies, our sophisticated protocol for peroxisome purification and the highly confident protein identifications are considered the major improvements toward reliable and comprehensive coverage of the plant peroxisomal proteome.

The horizontal spot pattern of several matrix enzymes is suggestive of charge-modifying posttranslational modifications, such as phosphorylation and acetylation, both of which are currently being investigated in greater detail. Some peroxisomal protein kinases are reported and several are predicted, along with phosphatases, to be matrix targeted (Fukao et al., 2002, 2003; Dammann et al., 2003; Reumann et al., 2004). Acetylation of internal Lys residues also decreases the pI of a polypeptide and has recently been recognized as an important regulatory signal in many cellular processes (for reviews, see Polevoda and Sherman, 2002; Fuchs et al., 2006). ATF2 (At1g77540; SSI>), whose x-ray structure has recently been resolved, is a minimal acetyl transferase of unknown subcellular localization (Tyler et al., 2006). We have now established its closely related homolog, ATF1 (At1g21770; SSI>; 80% identical with ATF1) as a novel constituent of plant peroxisomes by multiple lines of evidence, including in vivo EYFP targeting studies (Figures 5C and 5D). Conservation of the novel PTS1 SSI> of ATF1 in ATF2 strongly suggests that the entire two-member protein family is peroxisomal in *Arabidopsis*. Protein acetylation may thus be an as yet unrecognized regulatory mechanism of plant peroxisomal enzymes. Proteins showing multiple horizontal spot patterns (see Supplemental Figure 2 online) are reasonable candidate substrates of ATF1.

Targeting Verification for Improving Targeting Prediction

By in silico analysis for conservation of the predicted PTS in homologous plant ESTs (Reumann, 2004), the peroxisome targeting function of the predicted PTS peptides was supported for 17 of 28 novel proteins (Table 2; see Supplemental Figure 3 online; Reumann et al., 2004). Exceptions included novel proteins, whose PTS1-like peptides were unaltered in homologous ESTs, and *Brassicaceae*-specific proteins. Notably, no evidence against peroxisomal targeting, for instance, acidic amino acid residues at any position of the tripeptide, was obtained for any of the proteins. By subcellular analysis of reporter protein fusions, peroxisome targeting of six out of seven representative novel proteins with predicted PTS1s was confirmed. Artificial localization data possibly caused by cDNA expression from the strong 35S cauliflower mosaic virus promoter were excluded by colocalization of the proteins of interest with a cyan fluorescent peroxisome marker, as applied in previous studies (Fulda et al., 2002; Goepfert et al., 2006; Ma et al., 2006). Three enzymes with β-oxidation–related annotations (SDRb, ECHIb, and HBCDH), a glutathione *S*-transferase (GSTT1), and three enzymes involved in NADP metabolism (IDH, 6PGL, and 6PGDH; see below) were conclusively established for plant peroxisomes. Only full-length EYFP-6PGDH remained cytosolic, possibly owing to interference of the EYFP tag with PTS1 exposure or posttranslational regulatory mechanisms. Nonetheless, this 6PGDH isoform is considered peroxisomal owing to its conserved PTS1 and functional PTS1 domain (SKI>; Figure 4N; Reumann et al., 2004), the lack of predicted N-terminal targeting signals, and its apparent absence in the proteomes of chloroplasts and mitochondria (Kruft et al., 2001; Millar et al., 2001; Peltier et al., 2002).

The large number of 11 proteins with PTS1-related peptides suggested their role as functional yet unknown PTS1s. The PTS1-like peptides SSL>, SSI>, and ASL> were previously absent from or below threshold in plant PTS1 sequences (Reumann, 2004), and experimental data argued against a targeting function of SSI> and SSL>. Conclusive experimental support for an allowance of Ser at position −2 in general had not been reported ([SACGT][RKHLN][LMIY]>, Mullen et al., 1997; [SACP][RK][LMI]>, Hayashi et al., 1997; [SACGTP][RKHLN][LMIY]>, Kragler et al., 1998). Peroxisome targeting of the three full-length fusion proteins and the corresponding PTS domain constructs (Figure 5) identified ECH2, EH3, and ATF1 conclusively as plant peroxisomal proteins and SSL>, SSI>, and ASL> as novel noncanonical plant PTS1 tripeptides. Full-length ECH2 had previously been shown to be peroxisomal (Goepfert et al., 2006). Our results on EH3 support earlier biochemical localization data on *Ricinus* epoxide hydrolase in glyoxysomes (Stark et al., 1995) and point to a physiological role of EH3 distinct from lipid mobilization in germinating seeds.

The primary structure of the novel PTS1 peptides and their remarkable frequency in the proteome of leaf peroxisomes (e.g.,

four SSL> proteins), in contrast with their rare abundance in previously known plant PTS1 proteins, raises further biological questions. For instance, which structural feature specifically allows Ser to replace the generally essential basic residue at position −2 in plants? The emerging abundance of SSL>, SSI>, or ASL> in leaf peroxisomal proteins may be partly attributed to our ability to now detect weakly expressed peroxisomal matrix proteins. We propose that the newfound noncanonical PTS1s occur preferentially in low-abundance matrix proteins because the tripeptides have a reduced affinity to the cytosolic PTS1 receptor PEX5 and lower the speed of cargo import into the matrix. The previously known major plant peroxisomal matrix proteins, by contrast, rely on highly efficient canonical PTS peptides to adjust the rate of protein import to the intensity of gene expression (G.E. Antonicelli and S. Reumann, unpublished data). Thus, the identification of low-abundance proteins appears to be of major importance to fully cover the natural variety of plant peroxisomal proteins and the range of functional PTS1/2 peptides in higher plants.

Even though our isolation method paves the way for analysis of other abundant peroxisome variants from *Arabidopsis*, it remains unrealistic to envision proteome studies of all plant microbody forms in the near future (e.g., from flowers, trichomes, stems, and roots). Prediction-based in silico studies will therefore remain the second major large-scale approach to fully describe the plant peroxisomal proteome. The prediction of plant peroxisomal proteins benefits significantly from the proteome data generated in the course of this study, in terms of both increased sensitivity and specificity. First, the three novel PTS1 peptides allow extended genome screens for putative PTS1 proteins and a significant enlargement of the database AraPerox (www.araperox.uni-goettingen.de; Table 3). The 100 additional new entries are predicted to include numerous interesting true peroxisomal proteins (for example, see Supplemental Figure 8 online) but may also comprise some false positives, if peroxisome targeting of some proteins depends on yet unknown enhancing elements. Experimental analysis of the predicted peroxisome targeting function of further PTS1-related peptides (e.g., GR, TNL>; METE1, SAK>; and NBP, SKV>) is expected to reveal further functional PTS1s.

Second, upon experimental verification of the targeting function of predicted PTS peptides, novel peroxisomal matrix proteins can be applied as input sequences to improve in silico predictions of PTS1/2 proteins. EYFP extended by the C-terminal domains of any of the 11 representative novel proteins showed a punctate distribution, conclusively demonstrating that the proteins carry functional PTS1s and use the PTS1 targeting pathway (Figure 4). In addition, peroxisome targeting of three other proteins identified in both *Arabidopsis* and spinach leaf peroxisomes has been confirmed for the corresponding full-length *Arabidopsis* homologs as EYFP fusion proteins (ECHIa, ECHId/NS, and SDRa) and their predicted targeting domains (SKL>, RLx_5HL, and SRL>, respectively; L. Babujee, V. Wurtz, C. Ma, F. Lueder, A. van Dorselaer, and S. Reumann, unpublished data). In summary, the characterization of 26 novel PTS1/2 proteins at the molecular level, combined with experimental definitions of their targeting signals as reported in this and previous studies of the past 3 years (12 additional proven or putative PTS1/2 proteins; see Introduction), represents a significant extension of the previous number of known matrix proteins applicable as input sequences for EST database searches and discriminative analyses of PTS1 domains. The data will make possible a more comprehensive definition of functional PTS peptides, the characterization of auxiliary targeting elements, and an investigation of any interdependence of these parameters in higher plants.

An Internal PTS2 in TLP

The characterization of a functional PTS2 in the *Arabidopsis* TLP is biologically significant because (1) eukaryotic transthyretin homologs previously have not been localized to peroxisomes and (2) eukaryotic proteins have not been demonstrated to bear functional PTS2s at an internal position. TLPs are homologous to the mammalian thyroid-transport protein transthyretin, but they lack hormone binding activity and are generally considered cytosolic. The proteome data and the subcellular reporter protein studies of native and modified EYFP constructs provide conclusive evidence for peroxisome targeting of full-length *Arabidopsis* TLP (Figures 2, 3, 5G, and 5H). The low import efficiency of EYFP-TLP may reflect conformation-limited accessibility of the internal PTS2 for PEX7 and/or its competition with another targeting signal, for instance, the yet unknown peptide that directed the inversely arranged full-length fusion protein, TLP-GFP, to the plasma membrane (Nam and Li, 2004).

Genome screens for PTS2 proteins should thus be extended beyond the N-terminal 40–amino acid domain (Table 3). Internal PTS2s, however, are thought to remain rare in nature and to occur preferentially in bifunctional proteins that evolved by gene fusion, as deduced for plant TLP, a predicted bifunctional enzyme of purine metabolism. The two catalytic domains of plant TLP were apparently fused shortly after the divergence of *Dictyostelium* in the plant lineage, to facilitate stoichiometric protein synthesis, peroxisome targeting, protein–protein interaction, and possibly metabolite channeling. Uricase, in fact, produces 5-hydroxyisourate (5-HIU) rather than the presumed pathway end product, allantoin. The enzyme that succeeds uricase in purine catabolism and opens the ring (i.e., 5-HIU hydrolase [COG2351]) turned out to be encoded by *tlp* (Figure 3A; Lee et al., 2005; Jung et al., 2006). The reaction product is converted to (*S*)-allantoin by a decarboxylase (COG3195; Ramazzina et al., 2006) that is homologous to the additional N-terminal domain of bifunctional *Arabidopsis* TLP (Figure 3). The likely role of *Arabidopsis* TLP in purine metabolism matches peroxisome targeting of full-length TLP_{324} to the same compartment as uricase. The shorter splice variants of plants lacking the PTS2 are probably cytosolic (e.g., $AtTLP_{311}$ and $AtTLP_{286}$; Figure 3A; see Supplemental Figure 3P online) and are expected to conduct distinct yet unknown physiological roles, possibly including hormone transport-related functions (e.g., in brassinosteroid signaling) (Nam and Li, 2004).

Peroxisomal Proteins Lacking Obvious PTSs Indicate Alternative Targeting Pathways

A significant number of the novel leaf peroxisomal proteins were expected to lack predicted PTS1/2 peptides (see Introduction).

Some of these proteins had previously been predicted (e.g., GR and OASS A1) or experimentally demonstrated to be cytosolic (METE1, Ravanel et al., 2004; ACAT2, Carrie et al., 2007). Biochemically isolated cytosolic fractions, however, generally contain a significant portion of soluble proteins deriving from lysed peroxisomes. Additionally, owing to an insufficient consideration of plant PTS1 peptides in most subcellular prediction programs, peroxisome targeting is often overlooked and excluded at the outset from common reporter constructs with C-terminal tags. Peroxisome targeting of a few proteins remains ambiguous. OZI1 has also been detected in isolated mitochondria, but the corresponding organelle fraction contained several plant peroxisomal enzymes (Heazlewood et al., 2004). As OZI1 was restricted to leaf peroxisomes of high purity in our study and lacks a predicted mitochondrial presequence, the protein is considered to be peroxisome targeted. By contrast, Mn-dependent superoxide dismutase (At3g10920) has been identified from a minor two-dimensional gel spot, whose intensity appeared to negatively correlate with leaf peroxisome purity. The predicted mitochondrial presequence and its reported targeting to mitochondria (del Rio et al., 2003; Heazlewood et al., 2004) require quantitative proteomics methods to conclusively address dual subcellular targeting.

Among the proteins lacking PTS-like peptides, the majority strikingly belong to two functional groups, defense-related proteins (the myrosinase and β-glucosidase system), or proteins associated with nucleic acid metabolism. The negative result of a control experiment investigating an artificial copurification of high molecular weight complexes strongly supports a physiologically relevant association of the proteins with leaf peroxisomes; the two RNA helicases RH11 and RH37 are potential exceptions (see Supplemental Figure 5 online). An artificial adherence of defense- and nucleic acid metabolism-related proteins to the peroxisomal membrane induced upon cell lysis is considered unlikely but is an inherent option of organellar proteome studies in general that cannot be excluded by any controls.

At first glance, the prediction of ER signal peptides in five out of seven defense-related proteins suggests an ER contamination; the lack of housekeeping ER proteins in the same fraction, however, excludes this option. Likewise, copurification of ER bodies, known to contain PYK10 as a major constituent, with leaf peroxisomes is unlikely because these wound-inducible organelles are hardly detectable in rosette leaves of standard plants (Matsushima et al., 2002). Also, leaf wounding by plant harvest was reduced to a minimum. We therefore propose an alternative pathway for targeting of these defense proteins to peroxisomes. Recent phylogenetic analyses suggest that peroxisomes stem from the ER (Gabaldon et al., 2006; Schluter et al., 2006), and few peroxisomal membrane proteins (e.g., plant APX and a viral protein) are delivered to peroxisomes via distinct ER subdomains (Lisenbee et al., 2003; McCartney et al., 2005). Specific soluble proteins, for instance, those that are glycosylated as they pass the ER, as are PYK10 and myrosinases (Halkier and Gershenzon, 2006), may thus enter the peroxisomal matrix also via the ER and possibly the Golgi. Two glycosylated plastidic proteins have likewise recently been shown to pass the ER (Villarejo et al., 2005; Nanjo et al., 2006). Alternatively, some glycoside hydrolases may be peripheral peroxisomal membrane proteins, as is PEN2/BGLU26 (Lipka et al., 2005).

The association of nucleic acid metabolism-related enzymes with peroxisomes, which are well known to lack DNA, RNA, and ribosomes, is first puzzling. Nevertheless, peroxisome targeting is supported by the considerable number of six proteins, their specific detection in leaf peroxisomes of highest purity, and the absence of cytosolic and nuclear contaminants from isolated leaf peroxisomes. In light of the specialization of peroxisomes in purine (i.e., adenine, guanosine) catabolism and our limited knowledge of the physiological role of most of these proteins, their participation in DNA and/or RNA degradation may be proposed. The lack of both recognizable PTSs and ER signal peptides suggests a second alternative targeting mechanism. In conclusion, numerous novel proteins identified in this proteome study and lacking conventional targeting signals suggest, apart from intriguing and often unexpected physiological functions, the existence of two different yet unknown targeting pathways for soluble proteins to peroxisomes and make possible straightforward follow-up studies.

Extended Physiological Functions of Leaf Peroxisomes in Fatty Acid β-Oxidation, Glutathione Metabolism, and Herbivore Defense

Consistent with our initial hypothesis, many novel proteins are indeed plant specific and afford valuable insights into novel metabolic and defense pathways of plant peroxisomes, three examples of which will be outlined in more detail. The superfamily of SDRs comprises important enzymes participating in metabolism of complex secondary metabolites (Kallberg and Persson, 2006). As plant peroxisomal family members had previously not been characterized, the five SDRs reported here indicate a major yet unexplored role of SDRs in leaf metabolism and fatty acid degradation. SDRa (At4g05530; SRL>) is predicted to be orthologous to the vertebrate peroxisomal NADP-dependent carbonyl reductase involved in retinol reduction in the framework of arachidonic acid metabolism (see Supplemental Table 3 online; Fransen et al., 1999). Developmental coexpression analysis suggests that peroxisomal NADP-dependent IDH (Figure 4) rather than the peroxisomal OPPP provides SDRa, for instance, during senescence, with NADPH (Zimmermann et al., 2004). SDRb (At3g12800; SKL>) is most likely the *Arabidopsis* ortholog of yeast and mammalian peroxisomal 2,4-dienoyl-CoA reductase (DECR), an auxiliary enzyme required for β-oxidation of unsaturated fatty acids (see Supplemental Table 3 online; Gurvitz et al., 1997; Fransen et al., 1999; Reumann et al., 2004). Even though sharing previously unpredicted atypical PTS1s and similar expression patterns (e.g., in flowers, during seed development), SDRc (At3g01980; SYM>) and SDRd (At3g55290; SSL>) are predicted to differ in cofactor specificity (see Supplemental Table 3 online). SDRd is related to a potato (*Solanum tuberosum*) SDR implicated in metabolism of a steroid-like compound that affects gibberellin homeostasis and tuberization (Bachem et al., 2001). Because both enzymatic domains of bifunctional BSMDR (At1g49670; SRL>) are homologous to monofunctional enzymes from mammals, the enzyme is proposed to catalyze two subsequent oxidations of a hydroxyl group and a double bond

of a steroid, phenylpropanoid derivative or lipid peroxidation product.

Pea plant peroxisomes contain GSH, whose primary function presumably is in ROS detoxification by the ascorbate-glutathione cycle (Jimenez et al., 1997, 1998). GR is the only GSH-dependent plant peroxisomal enzyme characterized biochemically. Pea GR has been partially purified, but peptide sequences have not been reported (del Rio et al., 2006; Romero-Puertas et al., 2006). With our identification of one peroxisomal GR isoform (At3g24170), dehydroascorbate reductase remains the last unknown cycle enzyme. Beyond GR, we identified two further GSH-dependent enzymes and are thus proposing multiple physiological roles of GSH in the peroxisomal matrix (see Supplemental Figure 7 online). Peroxisome targeting of GSTT1 (At5g41210; SKI>) has been demonstrated by three independent lines of evidence (Table 2, Figures 4K and 4L). The constitutive expression of *GSTT1* and the high glutathione peroxidase activity of the recombinant enzyme (Wagner et al., 2002) suggest a physiological function in endogenous rather than stress metabolism, for instance, in detoxification of lipid peroxidation products. Alternatively, and in the context of the identification of two enzymes of Cys and Met biosynthesis in leaf peroxisomes (OASS A1 and METE1; Table 2), GSTT1 may also relate to sulfur amino acid metabolism, similar to yeast peroxisomal GST ω (Barreto et al., 2006). The single *Arabidopsis* HMGDH (At5g43940) associates plant peroxisomes with formaldehyde detoxification. The enzyme is central to the two- to three-step pathway, the major physiological and presumably cytosolic route for detoxification of the cytotoxic agent in plants. Interestingly, recombinant HMGDH also reveals high activity with *S*-nitrosoglutathione (Sakamoto et al., 2002; Diaz et al., 2003), possibly representing the missing link between plant peroxisomes and NO signaling (del Rio et al., 2002).

Few but comprehensive recent studies indicate that peroxisomes are substantially involved in plant defense against pathogen attack (Taler et al., 2004; Koh et al., 2005; Lipka et al., 2005). These mechanisms currently lack counterparts in yeast and mammals and point to plant-specific peroxisomal functions that evolved in sessile organisms. The *Arabidopsis* homolog of human macrophage MIF (At3g51660; SKL>) is most likely another player in the self-protection of plants. Human MIF reveals a wide array of cellular defensive effects, for instance, in immune responses (Sun et al., 1996; for review, see Calandra and Roger, 2003; Thiele and Bernhagen, 2005). As eukaryotic MIF homologs have previously not been localized to peroxisomes, *Arabidopsis* will be ideal for studying functional specification of MIF paralogs in peroxisomal defense mechanisms.

Lipka et al. (2005) identified PEN2 as a peroxisomal member of the superfamily of glycoside hydrolases (family 1; pfam00232; see Supplemental Figure 8 online) and characterized the protein as part of an inducible preinvasion resistance system. β-D-glucosidases are involved in a wide array of biological functions; apart from lignification and hormone level homeostasis, the enzymes play a major role in chemical defense against pathogens and herbivores (Xu et al., 2004), as best exemplified by myrosinases, also referred to as TGGs. Myrosinases hydrolyze glucosinolates (β-thioglucoside-*N*-hydroxysulfates) (i.e., sulfur-rich glucoside derivatives) and are among the most prominent defense compounds to liberate bioactive isothiocyanates, nitriles, or epithionitriles with a wide range of biological activities in plant–herbivore and plant–pathogen interactions (Kliebenstein et al., 2005; Grubb and Abel, 2006; Halkier and Gershenzon, 2006). TGG1 (At5g26000) and TGG2 (At5g25980), identified here along with their regulatory subunit ESM1, are the two major myrosinases in above-ground tissue with major redundant function in glucosinolate breakdown and insect defense, all of which had previously not been linked to peroxisomes (Barth and Jander, 2006). Myrosinase activity is regulated by ESM1, which represses nitrile formation relative to isothiocyanate production (Zhang et al., 2006). In addition to two further glycoside hydrolases identified in leaf peroxisomes (BGL1, At1g52400; and PYK10, see Results), five glycoside hydrolases are predicted to be targeted to peroxisomes (Xu et al., 2004). The characterization of SSL> as a functional PTS1 (Figures 5A and 5B) enables recognition of another entire clade of putative peroxisomal isoforms (see Supplemental Figure 8 online). In summary, our proteome data further support the emerging defense function of plant peroxisomes against pathogens and indicate a protective role of the organelle against herbivory by insects. Future studies need to conclusively demonstrate targeting of these defense-related proteins to peroxisomes, unravel the proposed ER-mediated biogenesis pathway, identify the glucoside substrates, and reveal their precise defense role.

METHODS

Plant Growth

Standard *Arabidopsis thaliana* ecotype Columbia-0 plants were grown for 3.5 to 4.5 weeks in a 16-h-light/8-h-dark cycle (light period 10 to 2 PM) at 22°C under a light intensity of 100 to 150 $\mu E\ m^{-2}\ s^{-1}$. For the isolation of leaf peroxisomes from senescent leaves, 4-week-old plants were subjected for 4 d to dark-induced senescence. Plants were harvested at the end of an extended dark period (18 h dark).

Isolation of Leaf Peroxisomes

Arabidopsis leaves were ground in grinding buffer (170 mM Tricine-KOH, pH 7.5, 1.0 M sucrose, 1% [w/v] BSA, 2 mM EDTA, 5 mM DTT, 10 mM KCl, and 1 mM $MgCl_2$) in the presence of protease inhibitors using a mortar and a pestle. The suspension was filtered, and chloroplasts were sedimented at 5000*g* (1 min, SS34 rotor). Approximately 20 mL of supernatant was loaded onto a Percoll density gradient prepared in TE buffer (20 mM Tricine-KOH, pH 7.5, and 1 mM EDTA) supplemented with 0.75 M sucrose and 0.2% (w/v) BSA underlaid by 36% sucrose (w/w) in TE buffer (top to bottom: 3 mL of 15% Percoll, 9 mL of 38% Percoll, 2 mL mixture of 38% Percoll, and 36% [w/w] sucrose at a ratio of 2:1 and 1:2, and 3 mL of 36% (w/w) sucrose in TE buffer). The Percoll gradients were centrifuged for 12 min at 10,500 rpm and 10 to 20 min at 15,000 rpm (SS34 rotor). For analytical purposes, the gradient was fractionated in 2-mL fractions and small aliquots frozen for enzymatic analyses. For preparative purposes, the peroxisome fractions at the bottom of the gradient of several Percoll gradients were combined, diluted in 36% (w/w) sucrose in TE buffer and sedimented by centrifugation (30 min, 15,000 rpm, SS34 rotor), yielding the leaf peroxisomal fraction LP-P1. The organelles were gently homogenized and loaded on top of a discontinuous sucrose density gradient (1 mL 41% [w/w], 1 mL 44% [w/w], 1 mL 46% [w/w], 2 mL 49% [w/w], 0.5 mL 51% [w/w], 1 mL 55% [w/w], and 1 mL 60% [w/w] in TE buffer) and ultracentrifuged (30 min to overnight, 25,000 rpm; Beckman SW40). For

analytical purposes, the gradient was fractionated in 1-mL fractions and small aliquots frozen for enzymatic analyses. For preparative purposes, the leaf peroxisome fraction LP-P2, visible as a sharp white band above 55% (w/w) sucrose, was harvested, supplemented with protease inhibitors, and stored in appropriate aliquots. For the analysis of an artificial copurification of high molecular weight complexes with leaf peroxisomes, sucrose was omitted from the grinding and washing buffer and leaves and the fraction corresponding to that of intact leaf peroxisomes worked up in an identical manner. The activities of marker enzymes and protein concentration were determined as described (Ma et al., 2006) or by the 2-D Quant Kit (GE Healthcare) using BSA as standard. The contamination C of leaf peroxisomes by mitochondria and chloroplasts was calculated based on the relative activities of the corresponding marker enzyme activities (e.g., $A_{fum.}$ [% of CE]) that were recovered in the leaf peroxisome fraction LP-P2 (or LP − P1) compared with the crude extract (CE) according to the following formulae (Table 1):

$$A_{fum.}(\%\ \text{of CE}) = \frac{A_{fum.}(\text{LP} - \text{P2}) \cdot 100}{A_{fum.}(\text{CE})}$$

$$C_{mitoch.} = \frac{100 \cdot A_{fum.}(\%\ \text{of CE})}{A_{HPR}(\%\ \text{of CE})}$$

2-DE

Improved protein solubilization was achieved in the presence of urea, thiourea, and zwitterionic detergents. The limited solubilization capabilities of 3-[(3-cholamidopropyl)-dimethylammonio]-1-propanesulfonate (CHAPS) were effectively compensated by the addition of amidosulfobetaine-14, though accompanied with a slight decrease in resolution in the first dimension as indicated by vertical smearing of high abundant proteins with basic pI, such as GOX (Figure 2). The proteins (200 to 500 μg) were precipitated (Wessel and Flügge, 1984), dissolved in IEF buffer (7 M urea, 2 M thiourea, 2% [w/v] CHAPS, 2% [w/v] amidosulfobetaine-14, and 0.5% IPG buffer; Destreak), the solution clarified by centrifugation (20 min, 16,000 xg), and the proteins subjected for ~60 kVh to isoelectric focusing (nonlinear Immobiline 18-cm pH gradient, pH 3.0 to 10). The proteins were then reduced and alkylated by equilibration for 12 min each in buffer (6 M urea, 50 mM Tris-HCl, pH 8.8, 30% [v/v] glycerol, 2% [w/v] SDS, and 0.001% [w/v] bromophenol blue) containing either 10 mg/mL DTT or 25 mg/mL iodoacetamide, respectively. For SDS-PAGE and the second dimension, the proteins were separated on large gradient gels (10 to 15% acrylamide) under denaturing conditions and stained with colloidal Coomassie Brilliant Blue.

Protein Identification from Two-Dimensional Gels

Manually excised gel plugs were processed as described in another recent large-scale proteome analysis (Werner et al., 2007). Briefly, an automated platform for the identification of gel-separated proteins (Jahn et al., 2006) was used to digest the proteins in gel with trypsin and to prepare the proteolytic peptides for MALDI-TOF-MS according to the thin layer affinity method. For each sample, a PMF spectrum and fragment ion spectra of up to four selected precursor ions were acquired within the same automated analysis loop using an Ultraflex I mass spectrometer (Bruker Daltonics). Database searches in the NCBI nonredundant primary sequence database restricted to the taxonomy of *Arabidopsis* were performed using the Mascot Software 2.0 (Matrix Science) licensed in house. Carboxamidomethylation of Cys residues was specified as fixed and oxidation of methionines as variable modification. One trypsin missed cleavage was allowed. Mass tolerances were set to 100 ppm for PMF searches and to 100 ppm (precursor ions) and 0.7 D (fragment ions) for MS/MS ion searches. Only proteins represented by at least one peptide sequence match above identity threshold in combination with the presence of at least four peptide masses assigned in the PMF were considered as identified.

LC-MS Shotgun Protein Analysis

Protein analysis was performed according to Wienkoop et al. (2004; see also detailed protocol in Morgenthal et al., 2007). Protein pellets (100 to 200 μg) were dissolved in 100 to 200 μL Lys-C solubilization buffer (50 mM Tris-HCl and 8 M Urea, pH 7.5) and digested with Endoproteinase Lys-C (Roche Applied Science) with an enzyme:substrate ratio of 1:1000 for 5 h at 37°C with gentle shaking. The digests were subsequently diluted fourfold with trypsin digestion buffer (50 mM Tris-HCl, 10% acetonitrile, and 10 mM $CaCl_2$, pH 7.5), resulting in a final concentration of 2 M urea. After addition of immobilized trypsin beads (Applied Biosystems) (enzyme:substrate ratio of 1:20), the samples were further incubated for 10 h at 37°C with gentle shaking. The digests were dissolved in 0.1% formic acid. Samples were concentrated on a precolumn and subsequently loaded onto a 15-cm silica-based C18 RP monolithic column (Merck Bioscience). Elution of the peptides was performed using a 2-h gradient from 100% solvent A (5% acetonitrile and 0.1% formic acid in water) to 100% solvent B (90% acetonitrile and 0.1% formic acid in water) using the Agilent nano HPLC system with a flow rate of 400 nL per min. Eluting peptides were analyzed with an LTQ mass spectrometer (Thermo Electron) operated in a data-dependent mode. Each full MS scan was followed by three MS/MS scans, in which the three most abundant peptide molecular ions were dynamically selected for collision-induced dissociation using a normalized collision energy of 35%. The temperature of the heated capillary and electrospray voltage was 150°C and 1.9 kV, respectively. After MS analysis, DTA files were created from raw files and searched against a database (http://www.arabidopsis.org/) using Bioworks 3.1 software (Thermo Fisher Scientific) using a precursor ion mass tolerance of 500 ppm, oxidized Met as dynamic modification, and fully tryptic peptides with one allowed miscleavage. With DTASelect, a list of identified proteins was obtained using the following criteria: Xcorr: −1 2.0, −2 2.2, and −3 3.5 for hits with at least two different peptides. Selected peroxisomal proteins found by a single peptide were postanalyzed manually and protein identification confirmed for 3 of 13 proteins (GOX3, BSMAR, and PYK10; Table 2). All the filtered and manually validated spectra are stored in a mass spectral reference library for plant proteomics called ProMEX (Hummel et al., 2007), which is accessible online (http://promex.mpimp-golm.mpg.de/). Using text query searches, for instance the Arabidopsis Genome Initiative code of the protein, it is possible to list all the corresponding product ion spectra. Unknown samples can be searched against the ProMEX library using dta, mfg, or mz data format files.

Subcellular Localization Analysis in *Allium cepa*

The full-length cDNA clones of IDH (At1g54340; SRL>) and 6PGL (At5g24400; SKL>) were cloned by RT-PCR using appropriate oligonucleotide primers (see Supplemental Table 4 online) as described previously for other cDNAs (Ma et al., 2006). ECHIb (At4g14430; PKL>), SDRb (At3g12800, previously At3g12790; SKL>), HBCDH (At3g15290; PRL>), 6PGDH (At3g02360; SKI>), GSTT1 (At5g41210; SKI>), ECH2 (At1g76150; SSL>), EH3 (At4g02340; ASL>), and TLP (At5g58220; internal RLx_5HL) were ordered from the ABRC. The cDNA of the minimal acetyltransferase 1 (ATF1; At1g21770; SSI>) was ordered from the RIKEN BioResource Center, and the missing N-terminal 12–amino acid residues were added by PCR (see Supplemental Table 4 online). The cDNAs were subcloned using appropriate oligonucleotide primers (see Supplemental Table 4 online) into pGEMT using the pGEM-T Easy vector system (Promega) or directly into pCAT-YFP-N-fus to fuse their 5′ end in frame with *EYFP*, under control of a double 35S cauliflower mosaic virus promoter (Fulda

et al., 2002; Ma et al., 2006). For 6PGL, the predicted transit peptide was omitted when fused 5′-terminally with *EYFP* (EYFP-6PGL). Site-directed mutagenesis was performed using PfuUltra high-fidelity (HF) DNA polymerase for mutagenic primer-directed replication of both plasmid strands of EYFP-TLP in pCAT-EYFP-Nfus using the Quick-Change II site-directed mutagenesis kit (Stratagene; see Supplemental Table 4 online). Thereby, the internal PTS2 (RLx_5HF) was mutated to the loss-of-function variant RLx_5DF. For analysis of the peroxisome targeting function of putative PTS domains, the C-terminal 10 residues of ECHIb, SDRb/DECR, HBCDH, IDH, 6PGDH, 6PGL, GSTT1, ECH2, EH3, and ATF1 were fused to the C terminus of EYFP by PCR using an extended reverse primer and subcloned likewise into pCAT, replacing the *EYFP* insert. In double transformants, peroxisomes were labeled with CFP as described previously (Fulda et al., 2002; Ma et al., 2006). Onion epidermal cells were transformed biolistically and the onion slices placed on wet paper in Petri dishes and stored on a benchtop for 16 to 24 h. For analysis by fluorescence microscopy, the onion skin epidermal cell layer was peeled and transferred to a glass slide. All subcellular analyses were reproduced at least three times in independent experiments. Fluorescence microscopy was performed as described (Ma et al., 2006).

Supplemental Data

The following materials are available in the online version of this article.

Supplemental Figure 1. Work Flow of the Isolation of Leaf Peroxisomes from Mature Leaves of *Arabidopsis* by Percoll and Sucrose Density Gradient Centrifugation.

Supplemental Figure 2. Detection of Specific Leaf Peroxisomal Matrix Enzymes in Multiple Spots and Upregulation of Defense-Related Proteins in Leaf Peroxisomes from Senescent Plants.

Supplemental Figure 3. PTS Conservation of Novel *Arabidopsis* Proteins Identified in Isolated Leaf Peroxisomes.

Supplemental Figure 4. Subcellular Targeting Analysis of 6PGL-EYFP in Onion Epidermal Cells.

Supplemental Figure 5. Analysis of a Copurification of High Molecular Weight Complexes with *Arabidopsis* Leaf Peroxisomes.

Supplemental Figure 6. Venn Diagram Comparing the Number of Proteins Identified in This and Previous Proteome Studies on *Arabidopsis* Peroxisomes.

Supplemental Figure 7. Model of Plant Peroxisomal Glutathione Metabolism.

Supplemental Figure 8. Phylogenetic Analysis of the *Arabidopsis* Glycoside Hydrolase Family 1.

Supplemental Table 1. Known Proteins of Plant Peroxisomes Identified in Isolated Leaf Peroxisomes from *Arabidopsis*.

Supplemental Table 2. MS Data of Proteins Identified.

Supplemental Table 3. Sequence Conservation of SDR Domains in Peroxisomal SDRs.

Supplemental Table 4. Cloning, Subcloning, and Mutagenesis Primers.

Supplemental Data Set 1. Amino Acid Sequence Alignments Used in Construction of the *Arabidopsis* Glycoside Hydrolase Family 1 Phylogenetic Tree in Supplemental Figure 8.

ACKNOWLEDGMENTS

We thank G. Gottschalk (Göttingen Genomics Center, Germany) and T. Pieler of the medical faculty for cDNA sequencing, I. Feuβner for the support of our research, M. Fulda for stimulating discussions, J.W. Kellmann (Max-Planck-Institute of Ecological Chemistry, Jena, Germany) for reading the manuscript, and A. Liavonchanka and G. Wieser for some cDNA subcloning work. We appreciate the editorial corrections and the help in SDR analysis provided by K. Bird (Plant Research Laboratory, Lansing, MI) and B. Persson (Karolinska Institutet, Stockholm, Sweden), respectively. cDNA provision by the ABRC and RIKEN is acknowledged. The research has been supported by grants from the Deutsche Forschungsgemeinschaft (RE1304/2 and RE1304/4) and by a Dorothea-Erxleben stipend from the government of Lower Saxony (to S.R.).

Received February 7, 2007; revised September 12, 2007; accepted September 24, 2007; published October 19, 2007.

REFERENCES

Arabidopsis Genome Initiative (2000). Analysis of the genome sequence of the flowering plant *Arabidopsis thaliana*. Nature **408:** 796–815.

Bachem, C.W., Horvath, B., Trindade, L., Claassens, M., Davelaar, E., Jordi, W., and Visser, R.G. (2001). A potato tuber-expressed mRNA with homology to steroid dehydrogenases affects gibberellin levels and plant development. Plant J. **25:** 595–604.

Barreto, L., Garcera, A., Jansson, K., Sunnerhagen, P., and Herrero, E. (2006). A peroxisomal glutathione transferase of *Saccharomyces cerevisiae* is functionally related to sulfur amino acid metabolism. Eukaryot. Cell **5:** 1748–1759.

Barth, C., and Jander, G. (2006). *Arabidopsis* myrosinases TGG1 and TGG2 have redundant function in glucosinolate breakdown and insect defense. Plant J. **46:** 549–562.

Beevers, H. (1979). Microbodies in higher plants. Annu. Rev. Plant Physiol. **30:** 159–193.

Calandra, T., and Roger, T. (2003). Macrophage migration inhibitory factor: A regulator of innate immunity. Nat. Rev. Immunol. **3:** 791–800.

Carrie, C., Murcha, M.W., Millar, A.H., Smith, S.M., and Whelan, J. (2007). Nine 3-ketoacyl-CoA thiolases (KATs) and acetoacetyl-CoA thiolases (ACATs) encoded by five genes in *Arabidopsis thaliana* are targeted either to peroxisomes or cytosol but not to mitochondria. Plant Mol. Biol. **63:** 97–108.

Corpas, F.J., Barroso, J.B., Sandalio, L.M., Distefano, S., Palma, J.M., Lupianez, J.A., and Del Rio, L.A. (1998). A dehydrogenase-mediated recycling system of NADPH in plant peroxisomes. Biochem. J. **330:** 777–784.

Corpas, F.J., Barroso, J.B., Sandalio, L.M., Palma, J.M., Lupianez, J.A., and del Rio, L.A. (1999). Peroxisomal NADP-dependent isocitrate dehydrogenase. Characterization and activity regulation during natural senescence. Plant Physiol. **121:** 921–928.

Dammann, C., Ichida, A., Hong, B., Romanowsky, S.M., Hrabak, E.M., Harmon, A.C., Pickard, B.G., and Harper, J.F. (2003). Subcellular targeting of nine calcium-dependent protein kinase isoforms from *Arabidopsis*. Plant Physiol. **132:** 1840–1848.

del Rio, L.A., Corpas, F.J., Sandalio, L.M., Palma, J.M., Gomez, M., and Barroso, J.B. (2002). Reactive oxygen species, antioxidant systems and nitric oxide in peroxisomes. J. Exp. Bot. **53:** 1255–1272.

del Rio, L.A., Sandalio, L.M., Altomare, D.A., and Zilinskas, B.A. (2003). Mitochondrial and peroxisomal manganese superoxide dismutase: Differential expression during leaf senescence. J. Exp. Bot. **54:** 923–933.

del Rio, L.A., Sandalio, L.M., Corpas, F.J., Palma, J.M., and Barroso, J.B. (2006). Reactive oxygen species and reactive nitrogen species in

peroxisomes. Production, scavenging, and role in cell signaling. Plant Physiol. **141:** 330–335.

Diaz, M., Achkor, H., Titarenko, E., and Martinez, M.C. (2003). The gene encoding glutathione-dependent formaldehyde dehydrogenase/GSNO reductase is responsive to wounding, jasmonic acid and salicylic acid. FEBS Lett. **543:** 136–139.

Dixon, D.P., Lapthorn, A., and Edwards, R. (2002). Plant glutathione transferases. Genome Biol. **3:** REVIEWS3004.

Dolferus, R., Osterman, J.C., Peacock, W.J., and Dennis, E.S. (1997). Cloning of the *Arabidopsis* and rice formaldehyde dehydrogenase genes: Implications for the origin of plant ADH enzymes. Genetics **146:** 1131–1141.

Edqvist, J., Ronnberg, E., Rosenquist, S., Blomqvist, K., Viitanen, L., Salminen, T.A., Nylund, M., Tuuf, J., and Mattjus, P. (2004). Plants express a lipid transfer protein with high similarity to mammalian sterol carrier protein-2. J. Biol. Chem. **279:** 53544–53553.

Emanuelsson, O., Elofsson, A., von Heijne, G., and Cristobal, S. (2003). *In silico* prediction of the peroxisomal proteome in fungi, plants and animals. J. Mol. Biol. **330:** 443–456.

Eneqvist, T., Lundberg, E., Nilsson, L., Abagyan, R., and Sauer-Eriksson, A.E. (2003). The transthyretin-related protein family. Eur. J. Biochem. **270:** 518–532.

Eriksson, S., Andreasson, E., Ekbom, B., Graner, G., Pontoppidan, B., Taipalensuu, J., Zhang, J., Rask, L., and Meijer, J. (2002). Complex formation of myrosinase isoenzymes in oilseed rape seeds are dependent on the presence of myrosinase-binding proteins. Plant Physiol. **129:** 1592–1599.

Eulalio, A., Behm-Ansmant, I., and Izaurralde, E. (2007). P bodies: At the crossroads of post-transcriptional pathways. Nat. Rev. Mol. Cell Biol. **8:** 9–22.

Fransen, M., Van Veldhoven, P.P., and Subramani, S. (1999). Identification of peroxisomal proteins by using M13 phage protein VI phage display: Molecular evidence that mammalian peroxisomes contain a 2,4-dienoyl-CoA reductase. Biochem. J. **340:** 561–568.

Fuchs, J., Demidov, D., Houben, A., and Schubert, I. (2006). Chromosomal histone modification patterns – From conservation to diversity. Trends Plant Sci. **11:** 199–208.

Fujiki, Y., Fowler, S., Shio, H., Hubbard, A.L., and Lazarow, P.B. (1982). Polypeptide and phospholipid composition of the membrane of rat liver peroxisomes: Comparison with endoplasmic reticulum and mitochondrial membranes. J. Cell Biol. **93:** 103–110.

Fukao, Y., Hayashi, M., Hara-Nishimura, I., and Nishimura, M. (2003). Novel glyoxysomal protein kinase, GPK1, identified by proteomic analysis of glyoxysomes in etiolated cotyledons of *Arabidopsis thaliana*. Plant Cell Physiol. **44:** 1002–1012.

Fukao, Y., Hayashi, M., and Nishimura, M. (2002). Proteomic analysis of leaf peroxisomal proteins in greening cotyledons of *Arabidopsis thaliana*. Plant Cell Physiol. **43:** 689–696.

Fulda, M., Shockey, J., Werber, M., Wolter, F.P., and Heinz, E. (2002). Two long-chain acyl-CoA synthetases from *Arabidopsis thaliana* involved in peroxisomal fatty acid beta-oxidation. Plant J. **32:** 93–103.

Gabaldon, T., Snel, B., van Zimmeren, F., Hemrika, W., Tabak, H., and Huynen, M.A. (2006). Origin and evolution of the peroxisomal proteome. Biol. Direct **1:** 8.

Geisbrecht, B.V., Zhang, D., Schulz, H., and Gould, S.J. (1999). Characterization of PECI, a novel monofunctional Delta(3), Delta(2)-enoyl-CoA isomerase of mammalian peroxisomes. J. Biol. Chem. **274:** 21797–21803.

Glinski, M., and Weckwerth, W. (2006). The role of mass spectrometry in plant systems biology. Mass Spectrom. Rev. **25:** 173–214.

Goepfert, S., Hiltunen, J.K., and Poirier, Y. (2006). Identification and functional characterization of a monofunctional peroxisomal enoyl-CoA hydratase 2 that participates in the degradation of even cis-unsaturated fatty acids in *Arabidopsis thaliana*. J. Biol. Chem. **281:** 35894–35903.

Goepfert, S., Vidoudez, C., Rezzonico, E., Hiltunen, J.K., and Poirier, Y. (2005). Molecular identification and characterization of the *Arabidopsis* delta(3,5),delta(2,4)-dienoyl-coenzyme A isomerase, a peroxisomal enzyme participating in the beta-oxidation cycle of unsaturated fatty acids. Plant Physiol. **138:** 1947–1956.

Goyer, A., Johnson, T.L., Olsen, L.J., Collakova, E., Shachar-Hill, Y., Rhodes, D., and Hanson, A.D. (2004). Characterization and metabolic function of a peroxisomal sarcosine and pipecolate oxidase from *Arabidopsis*. J. Biol. Chem. **279:** 16947–16953.

Gross, J., Cho, W.K., Lezhneva, L., Falk, J., Krupinska, K., Shinozaki, K., Seki, M., Herrmann, R.G., and Meurer, J. (2006). A plant locus essential for phylloquinone (vitamin K1) biosynthesis originated from a fusion of four eubacterial genes. J. Biol. Chem. **281:** 17189–17196.

Grubb, C.D., and Abel, S. (2006). Glucosinolate metabolism and its control. Trends Plant Sci. **11:** 89–100.

Gurvitz, A., Rottensteiner, H., Kilpelainen, S.H., Hartig, A., Hiltunen, J.K., Binder, M., Dawes, I.W., and Hamilton, B. (1997). The *Saccharomyces cerevisiae* peroxisomal 2,4-dienoyl-CoA reductase is encoded by the oleate-inducible gene SPS19. J. Biol. Chem. **272:** 22140–22147.

Halkier, B.A., and Gershenzon, J. (2006). Biology and biochemistry of glucosinolates. Annu. Rev. Plant Biol. **57:** 303–333.

Hawkins, J., and Boden, M. (2006). Detecting and sorting targeting peptides with neural networks and support vector machines. J. Bioinform. Comput. Biol. **4:** 1–18.

Hayashi, M., Aoki, M., Kondo, M., and Nishimura, M. (1997). Changes in targeting efficiencies of proteins to plant microbodies caused by amino acid substitutions in the carboxy-terminal tripeptide. Plant Cell Physiol. **38:** 759–768.

Hayashi, M., and Nishimura, M. (2006). *Arabidopsis thaliana* – A model organism to study plant peroxisomes. Biochim. Biophys. Acta **1763:** 1382–1391.

Heazlewood, J.L., Tonti-Filippini, J.S., Gout, A.M., Day, D.A., Whelan, J., and Millar, A.H. (2004). Experimental analysis of the *Arabidopsis* mitochondrial proteome highlights signaling and regulatory components, provides assessment of targeting prediction programs, and indicates plant-specific mitochondrial proteins. Plant Cell **16:** 241–256.

Helm, M., Luck, C., Prestele, J., Hierl, G., Huesgen, P.F., Frohlich, T., Arnold, G.J., Adamska, I., Gorg, A., Lottspeich, F., and Gietl, C. (2007). Dual specificities of the glyoxysomal/peroxisomal processing protease Deg15 in higher plants. Proc. Natl. Acad. Sci. USA **104:** 11501–11506.

Hennebry, S.C., Law, R.H., Richardson, S.J., Buckle, A.M., and Whisstock, J.C. (2006b). The crystal structure of the transthyretin-like protein from *Salmonella dublin*, a prokaryote 5-hydroxyisourate hydrolase. J. Mol. Biol. **359:** 1389–1399.

Hennebry, S.C., Wright, H.M., Likic, V.A., and Richardson, S.J. (2006a). Structural and functional evolution of transthyretin and transthyretin-like proteins. Proteins **64:** 1024–1045.

Hummel, J., Niemann, M., Wienkoop, S., Schulze, W., Steinhauser, D., Selbig, J., Walther, D., and Weckwerth, W. (2007). ProMEX: A mass spectral reference database for proteins and protein phosphorylation sites. BMC Bioinformatics **8:** 216.

Jahn, O., Hesse, D., Reinelt, M., and Kratzin, H.D. (2006). Technical innovations for the automated identification of gel-separated proteins by MALDI-TOF mass spectrometry. Anal. Bioanal. Chem. **386:** 92–103.

Jimenez, A., Hernandez, J.A., Del Rio, L.A., and Sevilla, F. (1997). Evidence for the presence of the ascorbate-glutathione cycle in

mitochondria and peroxisomes of pea leaves. Plant Physiol. **114:** 275–284.

Jimenez, A., Hernandez, J.A., Pastori, G., del Rio, L.A., and Sevilla, F. (1998). Role of the ascorbate-glutathione cycle of mitochondria and peroxisomes in the senescence of pea leaves. Plant Physiol. **118:** 1327–1335.

Johnson, T.W., Zybailov, B., Jones, A.D., Bittl, R., Zech, S., Stehlik, D., Golbeck, J.H., and Chitnis, P.R. (2001). Recruitment of a foreign quinone into the A1 site of photosystem I. In vivo replacement of plastoquinone-9 by media-supplemented naphthoquinones in phylloquinone biosynthetic pathway mutants of *Synechocystis* sp. PCC 6803. J. Biol. Chem. **276:** 39512–39521.

Jung, D.K., Lee, Y., Park, S.G., Park, B.C., Kim, G.H., and Rhee, S. (2006). Structural and functional analysis of PucM, a hydrolase in the ureide pathway and a member of the transthyretin-related protein family. Proc. Natl. Acad. Sci. USA **103:** 9790–9795.

Kallberg, Y., and Persson, B. (2006). Prediction of coenzyme specificity in dehydrogenases/reductases. A hidden Markov model-based method and its application on complete genomes. FEBS J. **273:** 1177–1184.

Kamada, T., Nito, K., Hayashi, H., Mano, S., Hayashi, M., and Nishimura, M. (2003). Functional differentiation of peroxisomes revealed by expression profiles of peroxisomal genes in *Arabidopsis thaliana*. Plant Cell Physiol. **44:** 1275–1289.

Kamigaki, A., Mano, S., Terauchi, K., Nishi, Y., Tachibe-Kinoshita, Y., Nito, K., Kondo, M., Hayashi, M., Nishimura, M., and Esaka, M. (2003). Identification of peroxisomal targeting signal of pumpkin catalase and the binding analysis with PTS1 receptor. Plant J. **33:** 161–175.

Kato, A., Takeda-Yoshikawa, Y., Hayashi, M., Kondo, M., Hara-Nishimura, I., and Nishimura, M. (1998). Glyoxysomal malate dehydrogenase in pumpkin: Cloning of a cDNA and functional analysis of its presequence. Plant Cell Physiol. **39:** 186–195.

Kikuchi, M., Hatano, N., Yokota, S., Shimozawa, N., Imanaka, T., and Taniguchi, H. (2004). Proteomic analysis of rat liver peroxisome: Presence of peroxisome-specific isozyme of Lon protease. J. Biol. Chem. **279:** 421–428.

Klein, A.T., van den Berg, M., Bottger, G., Tabak, H.F., and Distel, B. (2002). *Saccharomyces cerevisiae* acyl-CoA oxidase follows a novel, non-PTS1, import pathway into peroxisomes that is dependent on Pex5p. J. Biol. Chem. **277:** 25011–25019.

Kliebenstein, D.J., Kroymann, J., and Mitchell-Olds, T. (2005). The glucosinolate-myrosinase system in an ecological and evolutionary context. Curr. Opin. Plant Biol. **8:** 264–271.

Koh, S., Andre, A., Edwards, H., Ehrhardt, D., and Somerville, S. (2005). *Arabidopsis thaliana* subcellular responses to compatible *Erysiphe cichoracearum* infections. Plant J. **44:** 516–529.

Koo, A.J., Chung, H.S., Kobayashi, Y., and Howe, G.A. (2006). Identification of a peroxisomal acyl-activating enzyme involved in the biosynthesis of jasmonic acid in *Arabidopsis*. J. Biol. Chem. **281:** 33511–33520.

Kragler, F., Lametschwandtner, G., Christmann, J., Hartig, A., and Harada, J.J. (1998). Identification and analysis of the plant peroxisomal targeting signal 1 receptor NtPEX5. Proc. Natl. Acad. Sci. USA **95:** 13336–13341.

Kruft, V., Eubel, H., Jansch, L., Werhahn, W., and Braun, H.P. (2001). Proteomic approach to identify novel mitochondrial proteins in *Arabidopsis*. Plant Physiol. **127:** 1694–1710.

Lee, K.H., Piao, H.L., Kim, H.Y., Choi, S.M., Jiang, F., Hartung, W., Hwang, I., Kwak, J.M., Lee, I.J., and Hwang, I. (2006). Activation of glucosidase via stress-induced polymerization rapidly increases active pools of abscisic acid. Cell **126:** 1109–1120.

Lee, Y., Lee, D.H., Kho, C.W., Lee, A.Y., Jang, M., Cho, S., Lee, C.H., Lee, J.S., Myung, P.K., Park, B.C., and Park, S.G. (2005). Transthyretin-related proteins function to facilitate the hydrolysis of 5-hydroxyisourate, the end product of the uricase reaction. FEBS Lett. **579:** 4769–4774.

Leterrier, M., Corpas, F.J., Barroso, J.B., Sandalio, L.M., and del Rio, L.A. (2005). Peroxisomal monodehydroascorbate reductase. Genomic clone characterization and functional analysis under environmental stress conditions. Plant Physiol. **138:** 2111–2123.

Link, A.J., Eng, J., Schieltz, D.M., Carmack, E., Mize, G.J., Morris, D.R., Garvik, B.M., and Yates III, J.R. (1999). Direct analysis of protein complexes using mass spectrometry. Nat. Biotechnol. **17:** 676–682.

Lipka, V., et al. (2005). Pre- and postinvasion defenses both contribute to nonhost resistance in *Arabidopsis*. Science **310:** 1180–1183.

Lisenbee, C.S., Heinze, M., and Trelease, R.N. (2003). Peroxisomal ascorbate peroxidase resides within a subdomain of rough endoplasmic reticulum in wild-type *Arabidopsis* cells. Plant Physiol. **132:** 870–882.

Lisenbee, C.S., Lingard, M.J., and Trelease, R.N. (2005). *Arabidopsis* peroxisomes possess functionally redundant membrane and matrix isoforms of monodehydroascorbate reductase. Plant J. **43:** 900–914.

Ma, C., Haslbeck, M., Babujee, L., Jahn, O., and Reumann, S. (2006). Identification and characterization of a stress-inducible and a constitutive small heat-shock protein targeted to the matrix of plant peroxisomes. Plant Physiol. **141:** 47–60.

Matsushima, R., Hayashi, Y., Kondo, M., Shimada, T., Nishimura, M., and Hara-Nishimura, I. (2002). An endoplasmic reticulum-derived structure that is induced under stress conditions in *Arabidopsis*. Plant Physiol. **130:** 1807–1814.

Maynard, E.L., Gatto, G.J., Jr., and Berg, J.M. (2004). Pex5p binding affinities for canonical and noncanonical PTS1 peptides. Proteins **55:** 856–861.

McCartney, A.W., Greenwood, J.S., Fabian, M.R., White, K.A., and Mullen, R.T. (2005). Localization of the tomato bushy stunt virus replication protein p33 reveals a peroxisome-to-endoplasmic reticulum sorting pathway. Plant Cell **17:** 3513–3531.

Millar, A.H., Sweetlove, L.J., Giege, P., and Leaver, C.J. (2001). Analysis of the *Arabidopsis* mitochondrial proteome. Plant Physiol. **127:** 1711–1727.

Morgenthal, K., Wienkoop, S., Wolschin, F., and Weckwerth, W. (2007). Integrative profiling of metabolites and proteins: Improving pattern recognition and biomarker selection for systems level approaches. Methods Mol. Biol. **358:** 57–75.

Mullen, R.T., Lee, M.S., Flynn, C.R., and Trelease, R.N. (1997). Diverse amino acid residues function within the type 1 peroxisomal targeting signal. Implications for the role of accessory residues upstream of the type 1 peroxisomal targeting signal. Plant Physiol. **115:** 881–889.

Nagano, A.J., Matsushima, R., and Hara-Nishimura, I. (2005). Activation of an ER-body-localized beta-glucosidase via a cytosolic binding partner in damaged tissues of *Arabidopsis thaliana*. Plant Cell Physiol. **46:** 1140–1148.

Nakamura, T., Yokota, S., Muramoto, Y., Tsutsui, K., Oguri, Y., Fukui, K., and Takabe, T. (1997). Expression of a betaine aldehyde dehydrogenase gene in rice, a glycinebetaine nonaccumulator, and possible localization of its protein in peroxisomes. Plant J. **11:** 1115–1120.

Nam, K.H., and Li, J. (2004). The *Arabidopsis* transthyretin-like protein is a potential substrate of BRASSINOSTEROID-INSENSITIVE 1. Plant Cell **16:** 2406–2417.

Nanjo, Y., Oka, H., Ikarashi, N., Kaneko, K., Kitajima, A., Mitsui, T., Munoz, F.J., Rodriguez-Lopez, M., Baroja-Fernandez, E., and

Pozueta-Romero, J. (2006). Rice plastidial N-glycosylated nucleotide pyrophosphatase/phosphodiesterase is transported from the ER-Golgi to the chloroplast through the secretory pathway. Plant Cell **18:** 2582–2592.

Neuberger, G., Maurer-Stroh, S., Eisenhaber, B., Hartig, A., and Eisenhaber, F. (2003a). Prediction of peroxisomal targeting signal 1 containing proteins from amino acid sequence. J. Mol. Biol. **328:** 581–592.

Neuberger, G., Maurer-Stroh, S., Eisenhaber, B., Hartig, A., and Eisenhaber, F. (2003b). Motif refinement of the peroxisomal targeting signal 1 and evaluation of taxon-specific differences. J. Mol. Biol. **328:** 567–579.

Nowak, K., Luniak, N., Witt, C., Wustefeld, Y., Wachter, A., Mendel, R.R., and Hansch, R. (2004). Peroxisomal localization of sulfite oxidase separates it from chloroplast-based sulfur assimilation. Plant Cell Physiol. **45:** 1889–1894.

Peck, S.C. (2005). Update on proteomics in *Arabidopsis*. Where do we go from here? Plant Physiol. **138:** 591–599.

Peltier, J.B., Emanuelsson, O., Kalume, D.E., Ytterberg, J., Friso, G., Rudella, A., Liberles, D.A., Soderberg, L., Roepstorff, P., von Heijne, G., and van Wijk, K.J. (2002). Central functions of the lumenal and peripheral thylakoid proteome of *Arabidopsis* determined by experimentation and genome-wide prediction. Plant Cell **14:** 211–236.

Polevoda, B., and Sherman, F. (2002). The diversity of acetylated proteins. Genome Biol **3:** reviews0006.

Ramazzina, I., Folli, C., Secchi, A., Berni, R., and Percudani, R. (2006). Completing the uric acid degradation pathway through phylogenetic comparison of whole genomes. Nat. Chem. Biol. **2:** 144–148.

Ravanel, S., Block, M.A., Rippert, P., Jabrin, S., Curien, G., Rebeille, F., and Douce, R. (2004). Methionine metabolism in plants: Chloroplasts are autonomous for *de novo* methionine synthesis and can import S-adenosylmethionine from the cytosol. J. Biol. Chem. **279:** 22548–22557.

Reumann, S. (2002). The photorespiratory pathway of leaf peroxisomes. In Plant Peroxisomes: Biochemistry, Cell Biology and Biotechnological Applications, A. Baker and I.A. Graham, eds (Dordrecht, The Netherlands: Kluwer Academic Publishers), pp. 141–189.

Reumann, S. (2004). Specification of the peroxisome targeting signals type 1 and type 2 of plant peroxisomes by bioinformatics analyses. Plant Physiol. **135:** 783–800.

Reumann, S., Ma, C., Lemke, S., and Babujee, L. (2004). AraPerox. A database of putative Arabidopsis proteins from plant peroxisomes. Plant Physiol. **136:** 2587–2608.

Reumann, S., and Weber, A.P. (2006). Plant peroxisomes respire in the light: Some gaps of the photorespiratory C2 cycle have become filled–others remain. Biochim. Biophys. Acta **1763:** 1496–1510.

Romero-Puertas, M.C., Corpas, F.J., Sandalio, L.M., Leterrier, M., Rodriguez-Serrano, M., Del Rio, L.A., and Palma, J.M. (2006). Glutathione reductase from pea leaves: Response to abiotic stress and characterization of the peroxisomal isozyme. New Phytol. **170:** 43–52.

Sakamoto, A., Ueda, M., and Morikawa, H. (2002). *Arabidopsis* glutathione-dependent formaldehyde dehydrogenase is an S-nitrosoglutathione reductase. FEBS Lett. **515:** 20–24.

Saleem, R.A., Smith, J.J., and Aitchison, J.D. (2006). Proteomics of the peroxisome. Biochim. Biophys. Acta **1763:** 1541–1551.

Schluter, A., Fourcade, S., Ripp, R., Mandel, J.L., Poch, O., and Pujol, A. (2006). The evolutionary origin of peroxisomes: An ER-peroxisome connection. Mol. Biol. Evol. **23:** 838–845.

Schneider, K., Kienow, L., Schmelzer, E., Colby, T., Bartsch, M., Miersch, O., Wasternack, C., Kombrink, E., and Stuible, H.P. (2005). A new type of peroxisomal acyl-coenzyme A synthetase from *Arabidopsis thaliana* has the catalytic capacity to activate biosynthetic precursors of jasmonic acid. J. Biol. Chem. **280:** 13962–13972.

Sharma, Y.K., and Davis, K.R. (1995). Isolation of a novel *Arabidopsis* ozone-induced cDNA by differential display. Plant Mol. Biol. **29:** 91–98.

Shockey, J.M., Fulda, M.S., and Browse, J. (2003). *Arabidopsis* contains a large superfamily of acyl-activating enzymes. Phylogenetic and biochemical analysis reveals a new class of acyl-coenzyme A synthetases. Plant Physiol. **132:** 1065–1076.

Staiger, D., Zecca, L., Wieczorek Kirk, D.A., Apel, K., and Eckstein, L. (2003). The circadian clock regulated RNA-binding protein AtGRP7 autoregulates its expression by influencing alternative splicing of its own pre-mRNA. Plant J. **33:** 361–371.

Stark, A., Houshmand, H., Sandberg, M., and Meijer, J. (1995). Characterization of the activity of fatty-acid epoxide hydrolase in seeds of castor bean (*Ricinus communis* L.). Planta **197:** 84–88.

Stotz, H.U., Pittendrigh, B.R., Kroymann, J., Weniger, K., Fritsche, J., Bauke, A., and Mitchell-Olds, T. (2000). Induced plant defense responses against chewing insects. Ethylene signaling reduces resistance of *Arabidopsis* against Egyptian cotton worm but not diamondback moth. Plant Physiol. **124:** 1007–1018.

Strassner, J., Schaller, F., Frick, U.B., Howe, G.A., Weiler, E.W., Amrhein, N., Macheroux, P., and Schaller, A. (2002). Characterization and cDNA-microarray expression analysis of 12-oxophytodienoate reductases reveals differential roles for octadecanoid biosynthesis in the local versus the systemic wound response. Plant J. **32:** 585–601.

Sun, H.W., Bernhagen, J., Bucala, R., and Lolis, E. (1996). Crystal structure at 2.6-Å resolution of human macrophage migration inhibitory factor. Proc. Natl. Acad. Sci. USA **93:** 5191–5196.

Taler, D., Galperin, M., Benjamin, I., Cohen, Y., and Kenigsbuch, D. (2004). Plant *eR* genes that encode photorespiratory enzymes confer resistance against disease. Plant Cell **16:** 172–184.

Taylor, S.W., Fahy, E., and Ghosh, S.S. (2003). Global organellar proteomics. Trends Biotechnol. **21:** 82–88.

Thiele, M., and Bernhagen, J. (2005). Link between macrophage migration inhibitory factor and cellular redox regulation. Antioxid. Redox Signal. **7:** 1234–1248.

Tilton, G.B., Shockey, J.M., and Browse, J. (2004). Biochemical and molecular characterization of ACH2, an acyl-CoA thioesterase from *Arabidopsis thaliana*. J. Biol. Chem. **279:** 7487–7494.

Turner, J.E., Greville, K., Murphy, E.C., and Hooks, M.A. (2005). Characterization of *Arabidopsis* fluoroacetate-resistant mutants reveals the principal mechanism of acetate activation for entry into the glyoxylate cycle. J. Biol. Chem. **280:** 2780–2787.

Tyler, R.C., Bitto, E., Berndsen, C.E., Bingman, C.A., Singh, S., Lee, M.S., Wesenberg, G.E., Denu, J.M., Phillips, G.N., Jr., and Markley, J.L. (2006). Structure of *Arabidopsis thaliana* At1g77540 protein, a minimal acetyltransferase from the COG2388 family. Biochemistry **45:** 14325–14336.

Villarejo, A., et al. (2005). Evidence for a protein transported through the secretory pathway en route to the higher plant chloroplast. Nat. Cell Biol. **7:** 1224–1231.

Wagner, U., Edwards, R., Dixon, D.P., and Mauch, F. (2002). Probing the diversity of the Arabidopsis glutathione S-transferase gene family. Plant Mol. Biol. **49:** 515–532.

Werner, H.B., et al. (2007). Proteolipid protein is required for transport of sirtuin 2 into CNS myelin. J. Neurosci. **27:** 7717–7730.

Wessel, D., and Flügge, U.I. (1984). A method for the quantitative recovery of protein in dilute solution in the presence of detergents and lipids. Anal. Biochem. **138:** 141–143.

Wienkoop, S., Zoeller, D., Ebert, B., Simon-Rosin, U., Fisahn, J., Glinski, M., and Weckwerth, W. (2004). Cell-specific protein profiling in *Arabidopsis thaliana* trichomes: Identification of trichome-located

proteins involved in sulfur metabolism and detoxification. Phytochemistry **65:** 1641–1649.

Xu, Z., Escamilla-Trevino, L., Zeng, L., Lalgondar, M., Bevan, D., Winkel, B., Mohamed, A., Cheng, C.L., Shih, M.C., Poulton, J., and Esen, A. (2004). Functional genomic analysis of *Arabidopsis thaliana* glycoside hydrolase family 1. Plant Mol. Biol. **55:** 343–367.

Zhang, Z., Ober, J.A., and Kliebenstein, D.J. (2006). The gene controlling the quantitative trait locus EPITHIOSPECIFIER MODIFIER1 alters glucosinolate hydrolysis and insect resistance in Arabidopsis. Plant Cell **18:** 1524–1536.

Zimmermann, P., Hirsch-Hoffmann, M., Hennig, L., and Gruissem, W. (2004). GENEVESTIGATOR. *Arabidopsis* microarray database and analysis toolbox. Plant Physiol. **136:** 2621–2632.

Zolman, B.K., Monroe-Augustus, M., Thompson, B., Hawes, J.W., Krukenberg, K.A., Matsuda, S.P., and Bartel, B. (2001). *chy1*, an *Arabidopsis* mutant with impaired beta-oxidation, is defective in a peroxisomal beta-hydroxyisobutyryl-CoA hydrolase. J. Biol. Chem. **276:** 31037–31046.

Zolman, B.K., Nyberg, M., and Bartel, B. (2007). IBR3, a novel peroxisomal acyl-CoA dehydrogenase-like protein required for indole-3-butyric acid response. Plant Mol. Biol. **64:** 59–72.